EFFECT OF TWO-STAGE AGING ON MICROSTRUCTURE OF 7075 ALUMINUM ALLOYS

RE-627

Final Report

April 1981

by

Jonn M. Papazian

Prepared Under Contract N00019-79-C-0285

for

Department of the Navy
Naval Air Systems Command
Washington, D.C. 10361

by

Research Department
Grumman Aerospace Corporation
Bethpage, New York 11714

EFFECT OF TWO-STAGE AGING ON MICROSTRUCTURE OF 7075 ALUMINUM ALLOYS

RE-627

Final Report

April 1981

Prepared Under Contract N00019-79-C-0285

for

Department of the Navy
Naval Air Systems Command
Washington, D.C. 10361

by

John M. Papazian
Research Department
Grumman Aerospace Corporation
Bethpage, New York 11714

Approved by Richard A. Scheuing
Richard A. Scheuing
Director of Research

UNCLASSIFIED

SECURITY CLASSIFICATION OF THIS PAGE (When Date Entered)

REPORT DOCUMENTATION PAGE

READ INSTRUCTIONS BEFORE COMPLETING FORM

1. REPORT NUMBER	2. GOVT ACCESSION NO. AD-A100466 / 3. RECIPIENT'S CATALOG NUMBER
4. TITLE (and Subtitle) Effect of Two-Stage Aging on Microstructure of 7075 Aluminum Alloys	5. TYPE OF REPORT & PERIOD COVERED Final Report
	6. PERFORMING ORG. REPORT NUMBER RE-627
7. AUTHOR(s) John M. Papazian	8. CONTRACT OR GRANT NUMBER(s) N00019-79-C-0285
9. PERFORMING ORGANIZATION NAME AND ADDRESS Grumman Aerospace Corporation South Oyster Bay Road Bethpage, New York 11714	10. PROGRAM ELEMENT, PROJECT, TASK AREA & WORK UNIT NUMBERS 12 571
11. CONTROLLING OFFICE NAME AND ADDRESS Department of the Navy Naval Air Systems Command Washington, DC 10361	12. REPORT DATE April 1981 / 13. NUMBER OF PAGES 42
14. MONITORING AGENCY NAME & ADDRESS (if different from Controlling Office)	15. SECURITY CLASS. (of this report) UNCLASSIFIED / 15a. DECLASSIFICATION/DOWNGRADING SCHEDULE

16. DISTRIBUTION STATEMENT (of this Report)

Approved for public release; distribution unlimited

17. DISTRIBUTION STATEMENT (of the abstract entered in Block 20, if different from Report)

18. SUPPLEMENTARY NOTES

19. KEY WORDS (Continue on reverse side if necessary and identify by block number)

Aging, microstructure, thermal analysis, aluminum alloy 7075

20. ABSTRACT (Continue on reverse side if necessary and identify by block number)

Differential scanning calorimetry (DSC) and transmission electron microscopy (TEM) were used to establish the microstructural effects of various multistage aging treatments on aluminum alloy 7075. DSC was used to characterize the matrix microstructure while TEM was used to characterize the grain boundary precipitates. The aging treatments were in five categories: isochronal pre-aging, isothermal pre-aging, final aging at 150°C, commercial type two-stage aging treatments, and retrogression and re-aging (RRA) treatments.

DD FORM 1 JAN 73 1473 EDITION OF 1 NOV 65 IS OBSOLETE S/N 0102-014-6601

UNCLASSIFIED 400165

SECURITY CLASSIFICATION OF THIS PAGE (When Date Entered)

For two-stage aging treatments in which the final aging was for 8 h at 150°C, pre-aging for 6 h at 90°C or equivalent treatments at 120°C. This is in agreement with the Pashley et al model of two-state aging. For two-stage treatments where the first aging treatment is 4 h at 95°C, increasing the final aging temperature from 150 to 155 or 160°C resulted in a significant increase in the amount of η' in the microstructure; variations in the pre-aging treatment has much less of an effect. It was found that the RRA heat treatment converts the T6, predominately G.P. zone microstructure, to a more stable T7 type of microstructure; but the RRA microstructure consists of smaller precipitates and is more heterogeneous than the T7. The major differences between the T6, two-stage T6, RRA and T73 microstructures appear to be in the relative proportions of G.P. zones, η' and η. The percentage of G.P. zones is greatest in T6, least in T73 and RRA, and intermediate in the two-stage T6. Based on these limited observations, the stress corrosion susceptibility of 7075 appears to be more influenced by the matrix microstructure than by the grain boundary precipitate size and spacing.

ABSTRACT

Differential scanning calorimetry (DSC) and transmission electron microscopy (TEM) were used to establish the microstructural effects of various multistage aging treatments on aluminum alloy 7075. DSC was used to characterize the matrix microstructure while TEM was used to characterize the grain boundary precipitates. The aging treatments were in five categories: isochronal pre-aging, isothermal pre-aging, final aging at 150°C, commercial type two-stage aging treatments, and retrogression and re-aging (RRA) treatments.

For two-stage aging treatments in which the final aging was for 8 h at 150°C, pre-aging for 6 h at 90°C produced a slightly finer and harder microstructure than longer treatments at 90°C or equivalent treatments at 120°C. This is in agreement with the Pashley et al model of two-stage aging. For two-stage treatments where the first aging treatment is 4 h at 95°C, increasing the final aging temperature from 150 to 155 or 160°C resulted in a significant increase in the amount of η' in the microstructure; variations in the pre-aging treatment had much less of an effect. It was found that the RRA heat treatment converts the T6, predominately G.P. zone microstructure, to a more stable T7 type of microstructure; but the RRA microstructure consists of smaller precipitates and is more heterogeneous than the T7. The major differences between the T6, two-stage T6, RRA and T73 microstructures appear to be in the relative proportions of G.P. zones, η' and η. The percentage of G.P. zones is greatest in T6, least in T73 and RRA, and intermediate in the two-stage T6. Based on these limited observations, the stress corrosion susceptibility of 7075 appears to be more influenced by the matrix microstructure than by the grain boundary precipitate size and spacing.

CONTENTS

ILLUSTRATIONS

TABLES

1. INTRODUCTION

1.1 BACKGROUND

The poor stress corrosion resistance of aluminum alloy 7075 has led to numerous attempts to circumvent this problem. Newer alloys in the Al-Zn-Mg family have been developed, and overaging techniques for 7075 have been devised. Despite significant activity in this area, an entirely satisfactory solution has not yet been obtained. Two recent attempts at property improvement for 7075 involve two-stage aging treatments (Ref 1) and a patented, retrogression and re-aging (RRA) treatment (Ref 2). These treatments aim at producing precipitate microstructures in 7075 which have strength levels equal to those of the commonly used T6 temper but a stress corrosion resistance which is equal to or greater than that of the T73 temper. The two-stage aging treatment of 6 h at 105°C followed by 8 h at 150°C has been reported to increase stress corrosion life by serveral hundred percent while conserving the same tensile properties as material aged for the conventional 24 h at 120°C (Ref 1). Likewise, the RRA treatment can increase the stress corrosion threshold stress up to three times the normal value in 7075-T6 (Ref 2).

The objective of this work was to quantitatively characterize the precipitate microstructures of 7075 after systematic variations in two-stage aging treatments in order to establish the manner in which these precipitates depend upon the aging parameters. The selected aging heat treatments centered around the two-stage aging treatment reported by Di Russo, et el (Ref 1 and 3) and the various two-stage commercial treatments for T6, T73 and T76 (Ref 4). In addition, a sample of 7075-T651 which had received the patented RRA treatment was evaluated. The matrix microstructural evaluations were performed using differential scanning calorimetry (DSC). In previous studies, DSC has been shown to be of use for rapid characterization of the microstructures of 7000 series aluminum alloys (Ref 5 and 6). Transmission electron microscopy (TEM) was employed to determine the nature of the grain boundary precipitate microstructures, and electrical conductivity (EC) and hardness were used to further characterize the material.

1.2 PREVIOUS WORK

The sequence of precipitate phases observed during the aging of the Al-Zn-Mg alloys has been extensively studied (Ref 7 - 10). The aging sequence is currently thought to be (Ref 9 and 11):

$$\text{supersaturated } \alpha \rightarrow \text{G.P. zones} \rightarrow \eta'' \rightarrow \eta' \rightarrow \eta.$$

The G.P. Zones are spherical and have a f.c.c. structure which is fully coherent with the matrix (Ref 7). The η'' phase is usually described as spherical and coherent, but with an ordered G.P. zone or hexagonal structure (Ref 8, 9 and 11). The η' phase is a partially coherent, plate like precipitate on {111} with a hexagonal structure (Ref 8 and 12). The stable η, $MgZn_2$, phase also has a hexagonal structure and can transform to a ternary cubic T phase after prolonged aging at high temperatures (Ref 8).

The temperatures at which the different phases form vary with the exact composition of the alloy. Most of the microstructural work has been performed on pure alloys. In general, G.P. zones are the first phase to form at low aging temperatures, $T \leq 75°C$. When it is detected, η'', is observed at intermediate aging temperatures (75 to 150°C) or after long term aging at low temperatures. It is not always included as part of the aging sequence (Ref 7 and 10). The η' phase is also observed in this same temperature range. The η phase generally occurs at higher temperatures; but the work of Gjønnes and Simensen (Ref 8) and DeArdo and Simensen (Ref 13) suggests that η' and η can both be present after aging at 100°C.

The microstructure of Al-Zn-Mg alloys after two-stage aging treatments has been studied using TEM by Lorimer and Nicholson (Ref 14) and by DeArdo and Simenson (Ref 13). The results of these studies show finer precipitate distributions after two-stage aging and have been interpreted on the basis of theories of two-stage aging developed by Lorimer and Nicholson (Ref 14) and by Pashley, et al (Ref 15). The Lorimer and Nicholson theory postulates that when the low temperature aging treatment is performed below $T_{G.P.}$, the highest temperature for G.P. zone precipitation, the G.P. zones thus formed whose diameters exceed a critical value will survive the up-quench to the second aging temperature and provide the nucleation sites for η'. The Pashley et al model is similar except that the precipitates formed at the higher temperatures are thought to nucleate on clusters that are inherited from the low temperature aging treatment. The clusters need not be G.P. zones and may

have the structure of the final precipitate. The Pashley et. al. model was thought by DeArdo and Siemensen (Ref 13) to provide the best explanation for their results, particularly because they thought η' and η were both present at the lower aging temperatures.

In addition to the work mentioned above, a considerable amount of work has been done on the aging of pure Al-Zn-Mg alloys using DSC. This work has been performed by groups working in Japan, France and Austria, and Hungary. The Japanese workers have studied the aging of Al-Zn-Mg (Ref 16), two-step aging of Al-Zn-Mg (Ref 17) and prolonged aging of Al-Zn-Mg (Ref 18). In all of these studies, the alloy used was a pure pseudo-binary Al-6 wt% $MgZn_2$ with a composition of 0.94 wt% Mg, 5.06 wt% Zn. The calorimetric experiments reported in these papers were very well done and several of the general observations appear to be applicable to 7075. However, since the alloy used was a pure material whose composition was nearer to that of a medium strength Al-Zn-Mg alloy such as 7011, most of the detailed observations are not applicable. In particular, Hirano showed that the structure produced during aging at 130°C was strongly influenced by a pre-aging treatment at low temperature. This does not seem to be true for 7075 aged at 120°C, as will be shown later. In addition, Hirano's assignment of specific reaction peaks to particular dissolution reactions was not confirmed by TEM, and some choices appear to be questionable.

The French and Austrian workers have also performed extensive calorimetric investigations of Al-Zn-Mg alloys (Ref 19). Once again, they have studied pure alloys whose compositions are very nearly 5 wt% Zn, 1 wt% Mg. As with the Japanese studies, many of their detailed observations do not appear to be applicable to 7075. The major differences appear to be shifts in the temperature ranges in which the various transition phases are observed and dissimilar nucleation behavior for G.P. zones. In an early study of 7039, 7075 and a pure Al-Zn-Mg alloy, Thompson (Ref 20) has documented some of these dissimilarities.

The Hungarian workers also used pure alloys, but a variety of compositions were chosen (Ref 21-23). None of their alloys contained copper or chromium, but they documented the presence of the η'' (or G.P. II) phase. They also arrived at a dissolution enthalpy of 2.9 J/g for one volume percent G.P. zones in a variety of Al-Zn-Mg alloys.

2. EXPERIMENTAL PROCEDURES

The starting material for this investigation was a 6 in. long piece of 1 in. thick by 48 in. wide plate of 7075-T651 which was provided by the Naval Air Systems Command. Samples were machined from this material by first bandsawing 1 in. x 48 in. x 0.1 in. thick slabs from the plate and then milling and cutting to produce 1 in. x 2 in. x 0.063 in. sample coupons. Thus, the 1 in. dimension was parallel to the short transverse direction of the plate, the 2 in. dimension was parallel to the long transverse direction and the 0.063 in. parallel to the longitudinal direction. These coupons were solution heat treated for 2 h at 482°C in flowing argon and drop quenched into room temperature water. They were then transferred to liquid nitrogen and stored at 77 K. Subsequent aging of the samples was performed in silicone oil baths controlled to ± 1°C.

After aging, the electrical conductivity and hardness of the samples were measured using standard techniques. DSC analyses were performed on hand punched, 7/32 in. diameter, discs using a DuPont 990 Thermal Analyser with a plug-in DSC cell. At least three DSC runs were made for each sample in order to establish reproducibility. All of the DSC runs started at room temperature, ended at 530°C and were made with a constant heating rate of 10°C/min. A pure aluminum disc of approximately equal mass was used as the reference. The thermal analyser was connected to a mini-computer with a suitable interface, and the data from each run were continuously stored. After a run was completed, the data were converted to heat capacity vs. temperature using a previously established calibration for the DSC cell. Subsequently, a linear baseline was subtracted from the data. This baseline represents the temperature dependent heat capacity of the aluminum rich solid solution and existing precipitates, and its value was in agreement with the Neumann-Kopp rule. The remainder, the differential heat capacity (ΔC_p), represents the heat associated with solid state reactions which occurred during the DSC run. The reaction peaks in the ΔC_p vs T curves can be characterized by a reaction enthalpy, ΔH_r, the area of the peak, which is proportional to the molar heat of dissolution or formation of the precipitate and its concentration; and by T_r, the peak temperature, which is the temperature of maximum reaction rate.

This technique and its application to microstructual characterization of 7000 series aluminum alloys has been described in greater detail elsewhere (Ref 5 and 6).

TEM specimens were prepared from 3 mm (0.14 in.) discs that were punched from a section of the original sample that had been hand ground to approximately 0.25 mm (0.01 in.) thickness. Final thinning was performed in a twin jet electropolisher using a one part nitric acid, two parts methanol electrolyte at -20°C. The thin foils were examined in a Phillips EM300 equipped with a goniometer stage. In order to determine the characteristics of the grain boundary precipitates, the thin foil was first rotated such that a grain boundary was aligned with the tilt axis, and then tilted such that the boundary plane was vertical (parallel to the incident beam). The foil was then tilted again by approximately 30 to 40° so that the precipitates in the grain boundary were visible, and the boundary was photographed. Since the angle between the grain boundary and the incident beam was known, the grain boundary area could be accurately calculated. The sizes and densities of the grain boundary precipitates were then measured from the electron micrographs as follows.

The grain boundary precipitates were generally small, circular platelets lying in the plane of the grain boundary, thus the parameters measured were: N, the total number of precipitates; N_A, the number of precipitates per unit area of grain boundary; $\bar{\ell}$, the average length of the precipitate particle along the grain boundary; and A_f, the area fraction of the grain boundary covered by precipitates. The length of the precipitate along the grain boundary was measured since this direction was the tilt axis of the foil and was therefore not distored by projection. The area fraction was calculated by assuming that the precipitate platelets were disc shaped and had an average diameter equal to $\bar{\ell}$.

A sample of the original T651 plate that had been RRA treated by Lockheed-California was also analysed. The sample was approximately 0.5 in. x 1 in. x 6 in. and had been taken from the section of the plate labeled 6B3. Specimens for DSC analysis were taken from the face of this sample and from the mid-thickness by slicing with a water cooled, diamond impregnated, crystal cutting saw. DSC was the only technique used to evaluate this material.

3. RESULTS

The aging treatments used in this study can be arranged into five groups for comparison purposes: isochronal pre-aging treatments, isothermal pre-aging treatment, final aging at 150°C, commercial type two-stage aging treatments and the retrogression and re-aging treatment. Results from the DSC analyses of the microstructures of these five groups of treatments will be presented in sequence. These will then be followed by the results of the TEM study of grain boundary microstructures.

3.1 ISOCHRONAL PRE-AGING TREATMENTS

Thermograms from samples that were aged for 4 h at 90, 95, and 100°C are shown in Fig. 1. All of the DSC measurements in this study ran from room temperature to 530°C, but in Fig. 1 only the interval between 50 and 300°C is shown. The higher temperature portions of the thermograms have been omitted from the figures because they show only the dissolution of the stable, η, phase and they were identical for all of the aging treatments used. Figure 1 shows a small, endothermic, dissolution peak near 150°C (Peak I) and a large, exothermic, precipitation peak near 225° (Peak II). Aging for 4 h at 90 or 95°C resulted in similar microstructures, but 4 h at 100°C resulted in a decreased ΔH_r and an increased T_r for both dissolution and precipitation. These changes are tabulated in Table 1 which also lists the hardness and electrical conductivity of these samples. Both the hardness and conductivity of these samples increased as the aging temperature increased. Aging for 4 h at 100°C caused the hardness to increase significantly more than aging at 90 or 95°C. Note that the hardness values measured throughout this work tended to be slightly lower than expected for commercial practice. This is thought to be due to the use of small samples and the absence of stretching or stress relieving treatments.

The results of aging for 6 h at 75, 85, 90, 95, 100, 105 or 120°C are shown in Fig. 2. The trends of these data are similar to those shown in Fig. 1. As the aging temperature increased, ΔH_r for both peaks decreased. Simultaneously, T_r for both peaks increased. Peak II, the formation peak, has two maxima (Peaks IIa and IIb) after the lower temperature aging treat-

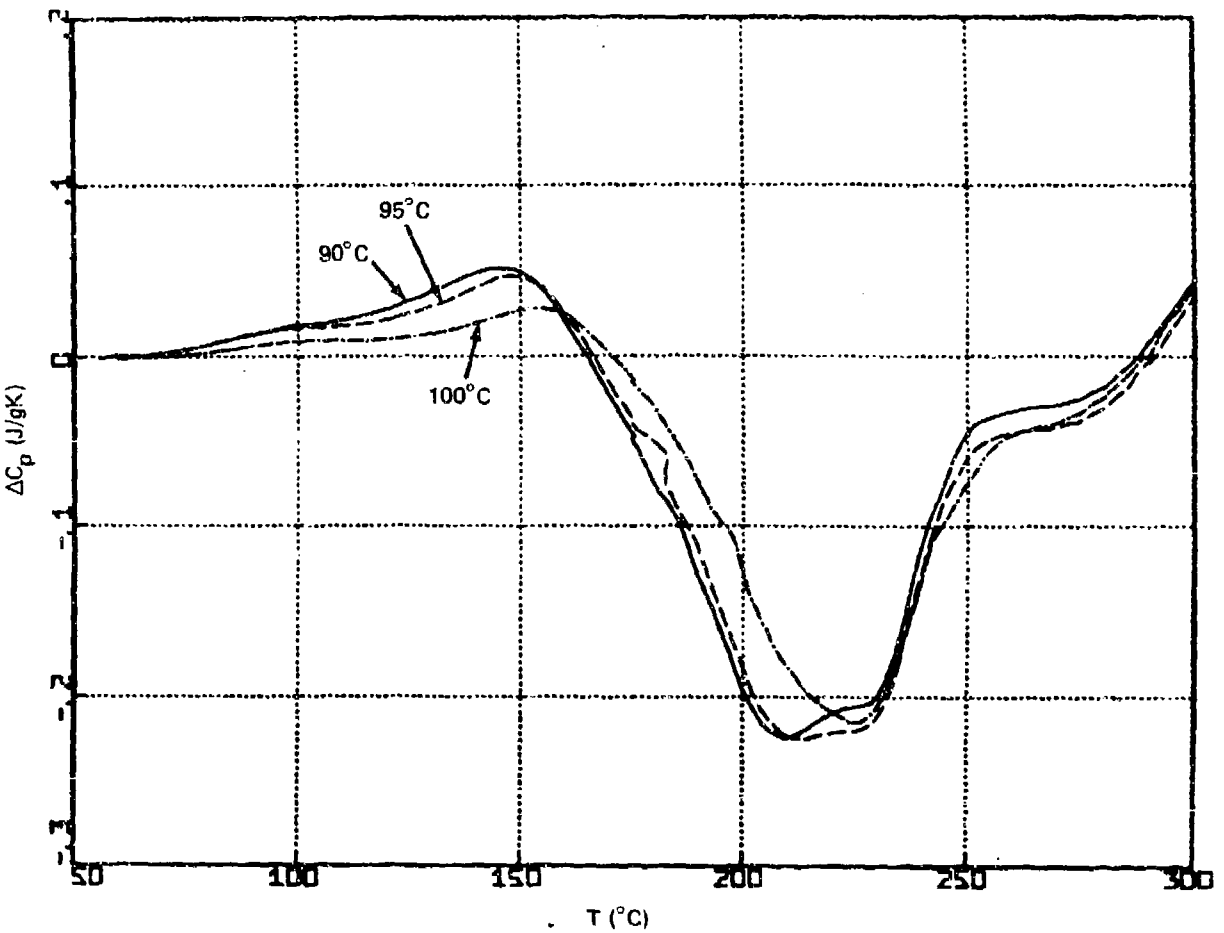

Fig. 1. DSC Traces From Solution Treated 7075 After Aging for 4 Hours at 90, 95 and 100°C.

Table 1. DSC Characteristics After Isochronal Pre-Aging Treatments

Aging				Peak I		Peak IIa		Peak IIb	
t (h)	T (°C)	Hardness (R_B)	EC (% IACS)	T_r (°C)	ΔH_r (J/g)	T_r (°C)	ΔH_r (J/g)	T_r (°C)	ΔH_r (J/g)
4	90	60±10	30.0	147	2.4±.1	211±2	-13.2±.4		
4	95	64±4	30.1	148	2.3±.2	215±3	-12.6±.9		
4	100	77±3	30.2	154	1.3±.1	224	-11.5±.1		
6	75	66±8	29.8	137±1	4.2±.5	208	-8.4±.2	228	-4.9±.6
6	85	72±2	30.0	149	3.0±.1	213±2	-12.7±.4		
6	90	65±2	30.8	146	3.1±.3	211±2	-7.4±.5	230	-4.4±.8
6	95	67±7	30.5	154	1.7±.4	225	-11.7±.3		
6	100	76±4	30.6	155	1.2±.4	225	-11.9±.5		
6	105	71±4	31.0	159	1.45±.3	225	-9.9±.4		
6	120	69±4	31.5	188	.31±.3	225	-7.5±.4		
8	95	76±4	30.3	156±2	2.0±.4	225	-11.4±.3		
8	100	70±4	31.0	159±1	.8±.2	226	-11.2±.2		
8	105	76±4	31.0	180	.9±.7	226±2	-9.3±.3		
8	110	76±3	31.3	174±7	.7±.5	227±1	-9.2±.3		

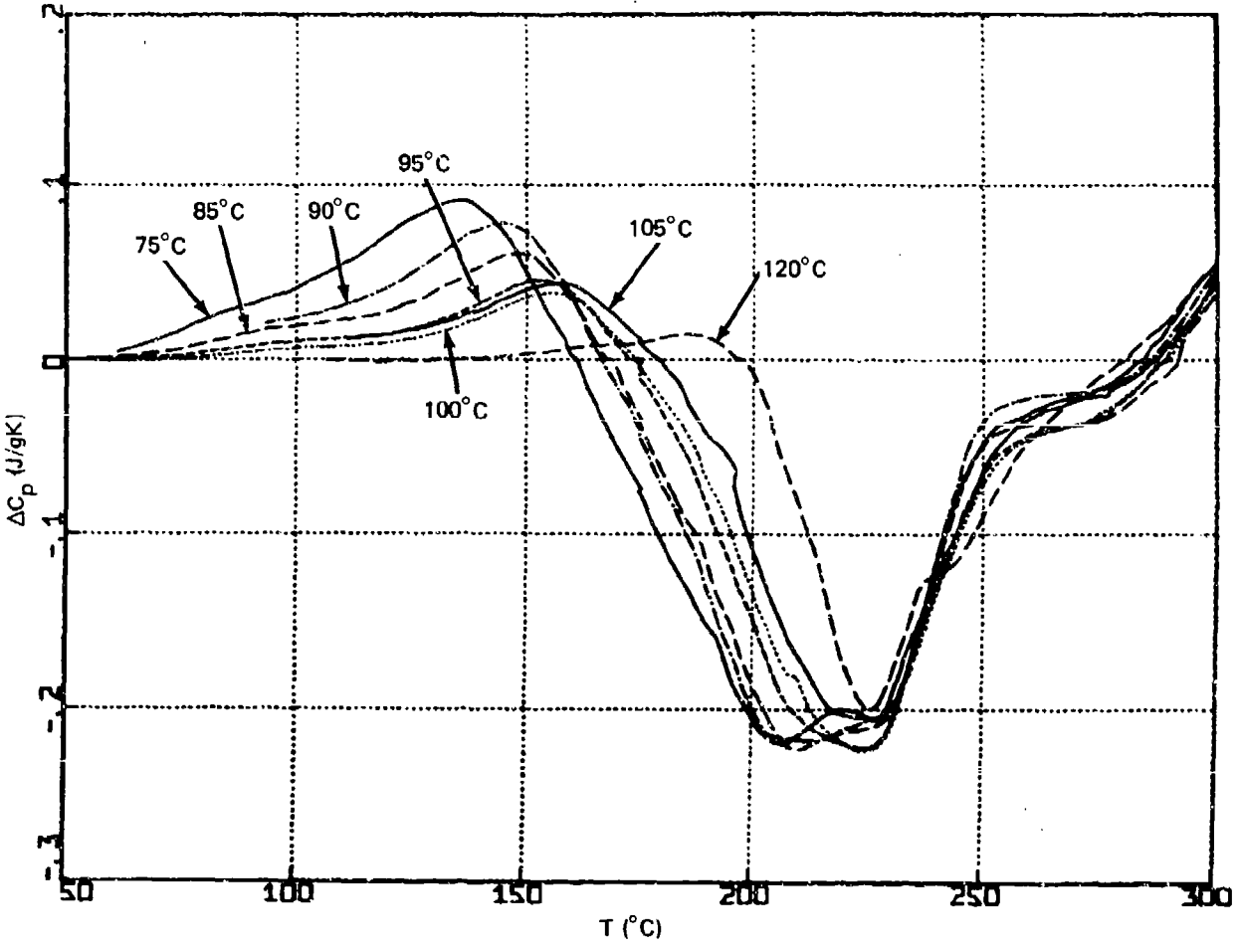

Fig. 2. DSC Traces From Solution Treated 7075 After Aging for 6 Hours at 75, 85, 90, 95, 100, 105 and 120°C.

ments, but evolves into a single peak after aging at the higher temperatures. (Note that the extrema appear as minima in the ΔC_p vs T plots but they are called maxima because they represent a maximum exothermic effect.) Values of the peak temperatures and enthalpies are given in Table 1, along with the hardness and conductivity. The conductivities of these samples increase as the aging temperature increases, but the hardness values have too much scatter to show a clear trend.

Results from the final series of isochronally pre-aged samples are shown in Fig. 3. Aging for 8 h at 95, 100, 105 and 110°C resulted in microstructural trends which are similar to the 4 and 6 h series. Peaks I and II both moved to slightly higher temperatures as the aging temperature increased, and their respective enthalpies decreased. The tabulated results in Table 1 show that the conductivities increased as the aging temperature increased but the hardness values did not change significantly.

3.2 ISOTHERMAL PRE-AGING TREATMENTS

The results of aging for 4, 6, 24, and 96 h at 90°C are shown in Fig. 4. Longer aging times resulted in an increased ΔH_r and T_r for Peak I. Concurrently, ΔH_r for Peak II decreased and T_r for Peak II increased. During these aging treatments, Peak II also evolved from a composite, double maxima, shape into a simpler peak with only one maximum. This change in shape of Peak II was also seen during isochronal aging, as previously shown in Fig. 1 and 2. Table 2 lists the characteristics of these samples after heat treatment. The hardness and conductivity both increased significantly as the aging time increased.

The results of aging for 4, 6, and 8 h at 95°C are shown in Fig. 5. Increased time at the aging temperature resulted in a small increase in T_r for Peak I and an evolution of the shape of Peak II. These changes were similar to those noted above for aging at 90°C but they were not as pronounced because of the smaller range of aging times studied. The results tabulated in Table 2 show the same general trends in hardness and conductivity as observed for aging at 90°C.

Figure 6 shows the results of aging for 4, 6, and 8 h at 100°C. As the aging time increased, there was a small decrease in the ΔH_r of Peak I

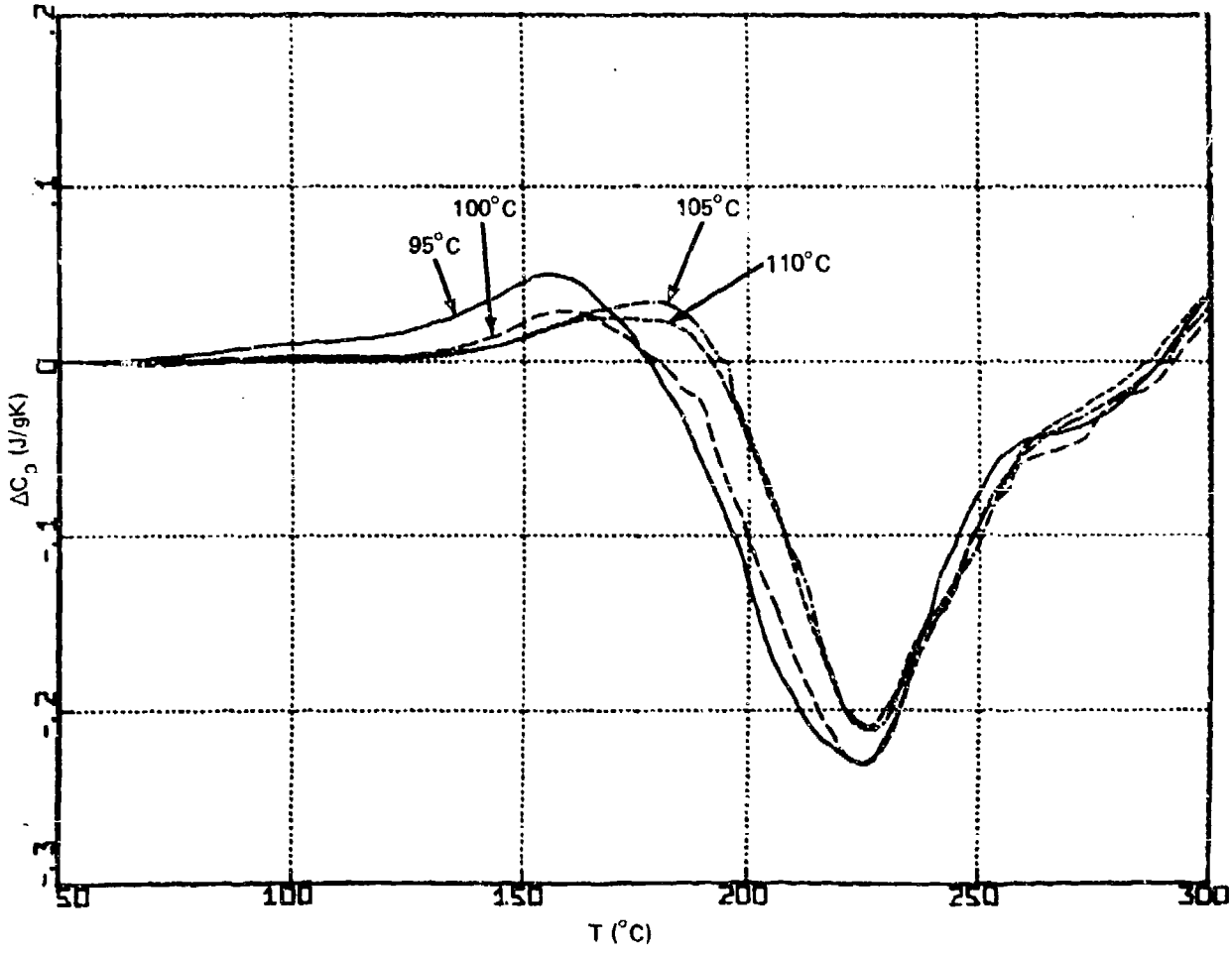

Fig. 3. DSC Traces From Solution Treated 7075 After Aging for 8 Hours at 95, 100, 105 and 110°C.

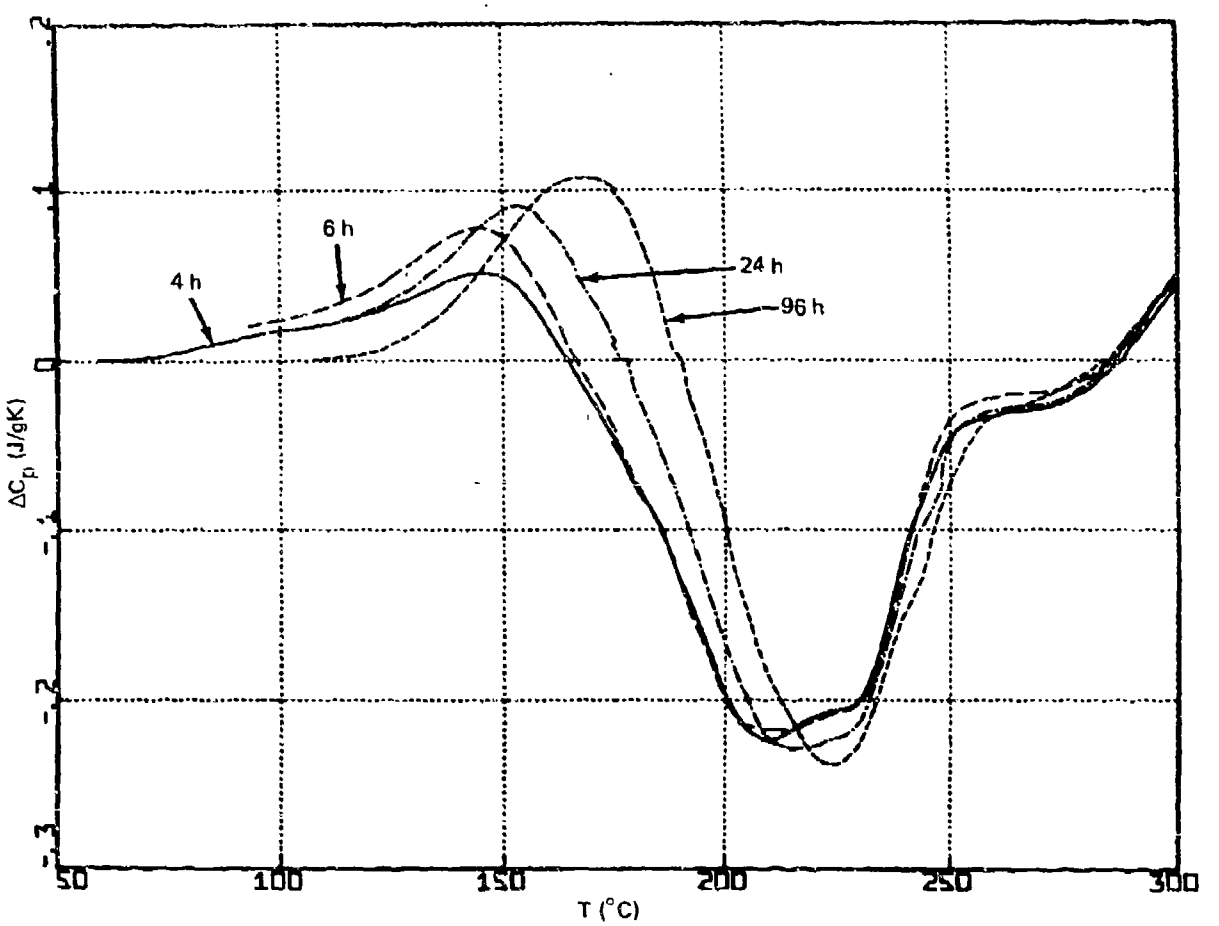

Fig. 4. DSC Traces From Solution Treated 7075 After Aging for 4, 6, 24 and 96 Hours at 90°C.

Table 2. DSC Characteristics After Isothermal Pre-Aging Treatments

Aging				Peak I		Peak IIa		Peak IIb	
t (h)	T (°C)	Hardness (R_B)	EC (% IACS)	T_r (°C)	ΔH_r (J/g)	T_r (°C)	ΔH_r (J/g)	T_r (°C)	ΔH_r (J/g)
4	90	60±10	30.0	147±1	2.4±.1	211±2	-13.2±.4		
6	90	65±2	30.8	146±1	3.1±.3	211±2	-7.4±.5	230±1	-4.4±.8
24	90	72±2	30.3	154±1	3.5±.1	218±5	-11.5±.8		
96	90	80±3	30.9	171±2	4.2±.2	224±2	-10.0±.5		
4	95	64±4	30.1	148±1	2.3±.2	215±3	-12.8±.9		
6	95	67±7	30.5	154±1	1.7±.4	225±1	-11.7±.3		
8	95	76±4	30.3	156±2	2.0±.4	225±1	-11.4±.3		
4	100	77±3	30.2	154±1	1.26±.1	224±1	-11.5±.1		
6	100	76±4	30.6	155±1	1.2±.4	225±1	-11.9±.5		
8	100	70±4	31.0	159±1	.8±.2	226±1	-11.2±.2		
6	120	69±4	31.5	188±1	.3±.3	225±1	-7.5±.4		
24	120	87±1	32.3	192±2	4.7±.3	227±1	-3.7±.3	246±3	-3.1±.1
96	120	86±1	33.0	192±2	5.9±.2	227±1	-2.6±.2	252±1	-2.7±.2

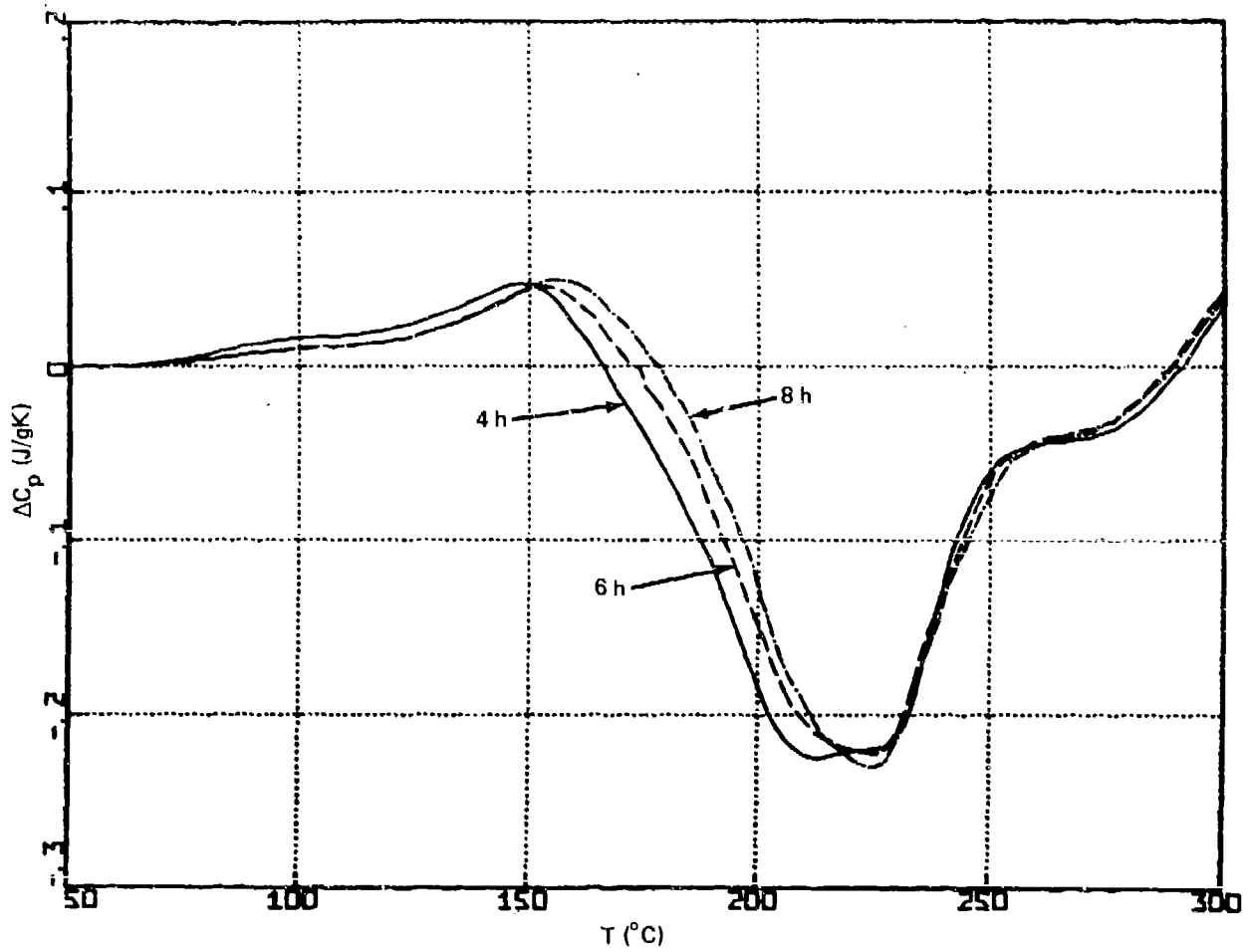

Fig. 5. DSC Traces From Solution Treated 7075 After Aging for 4, 6 and 8 Hours at 95°C.

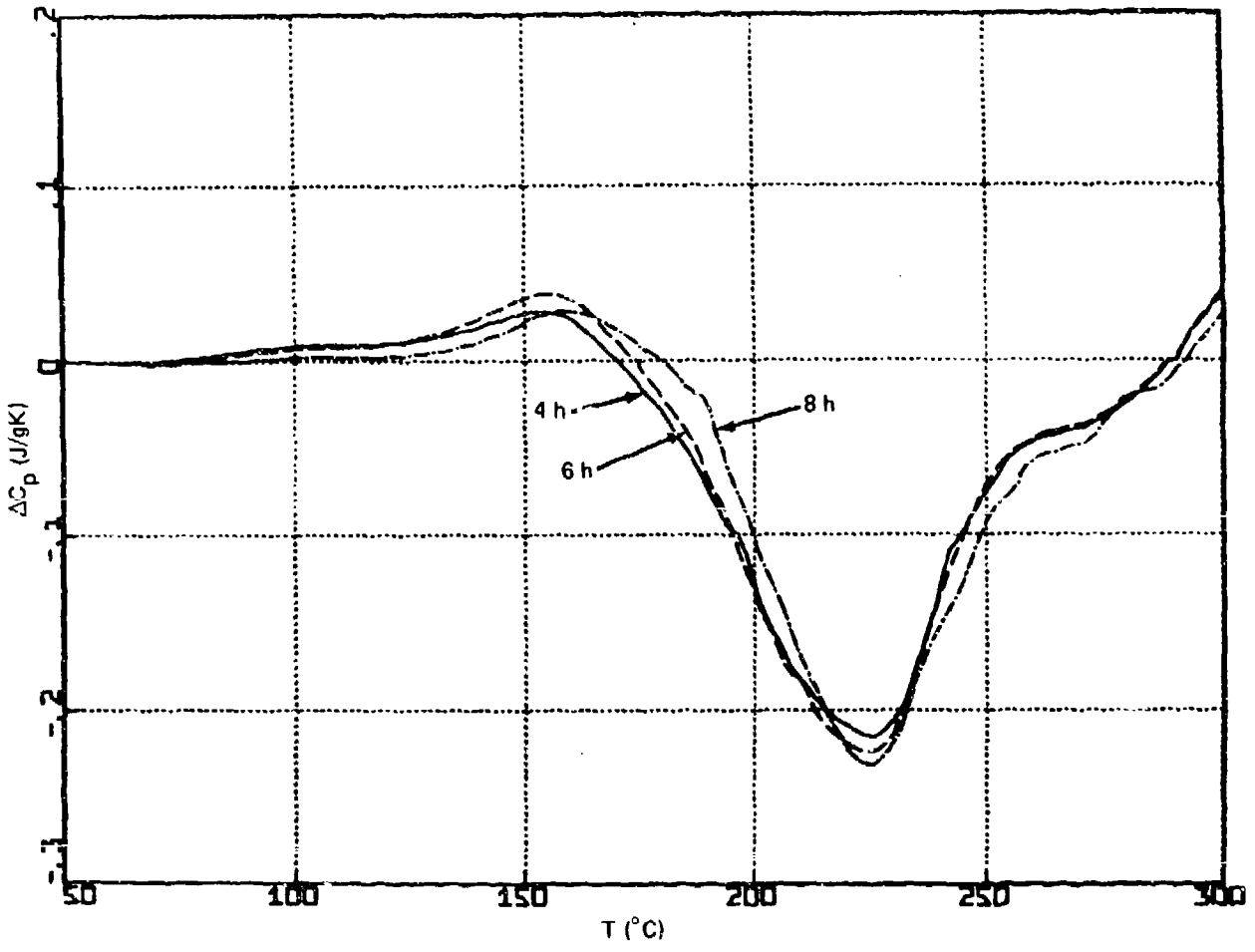

Fig. 6. DSC Traces From Solution Treated 7075 After Aging for 4, 6 and 8 Hours at 100°C.

coupled with a slight increase of T_r. There was virtually no change in Peak II. Conductivity increased as aging progressed but the hardness apparently decreased. The decrease in hardness is approximately equal to the scatter in the hardness measurements and may not be significant.

Figure 7 shows the result of aging at 120°C. After 6 h aging, Peak I is virtually non-existent. After 24 or 96 h, however, Peak I shows a large ΔH_r and a constant T_r of 192°C. The data in Table 2 shows that the ΔH_r after aging for 24 or 96 h was greater than in any of the previous aging treatments. This is consistent with the increased diffusivity of solute atoms at the higher aging temperature. The T_r for Peak I is also significantly higher than in any of the previous aging treatments. Peak II appears relatively sharp and displays a single maximum near 225°C after 6 h aging at 120°C. As aging proceeds, however, the shoulder on the high temperature side of the peak develops into a second peak. Note that the formation peaks with double maxima which were observed after the previously described lower temperature aging treatments had their second maximum located near 210°C, on the lower temperature side of the main 225°C peak, while the secondary maximum which develops after aging at 120°C is on the high temperature side, near 250°C. The maximum which develops near 250°C appears to be an additional formation reaction since the ΔC_p curve after 24 h aging lies below the 6 h curve. The hardness and conductivity both increase significantly during aging at 120°C.

3.3 150°C SECOND AGING TREATMENT

A second aging treatment of 8 h at 150°C was applied to several sets of the pre-aged samples. The first set of treatments consisted of 6, 24, and 96 h at 90°C followed by 8 h at 150°C. Results of DSC analysis of these three microstructures are shown in Fig. 8 and tabulated in Table 3. The results show that the microstructures were all quite similar, but ΔH_r and T_r for Peak I decreased slightly as the aging time at 90°C increased. Concurrently, ΔH_r for Peaks IIa and IIb increased and the hardness of the samples decreased slightly.

Similar trends were observed after aging for 6, 24, and 96 h at 120°C before aging 8 h at 150°C. The results in Fig. 9 and Table 3 show that the microstructures were similar but there might have been a slight decrease in

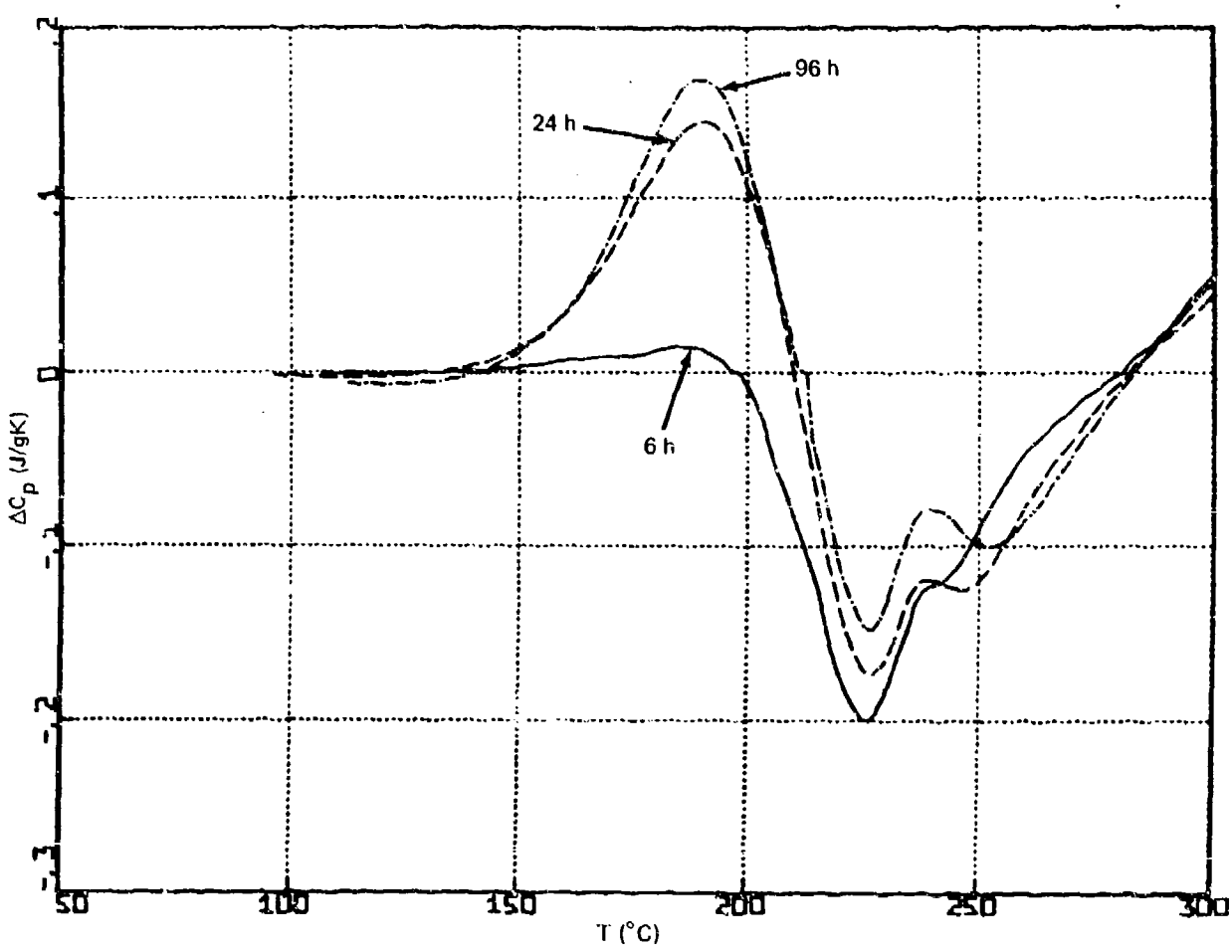

Fig. 7. DSC Traces From Solution Treated 7075 After Aging for 6, 24 and 96 Hours at 120°C.

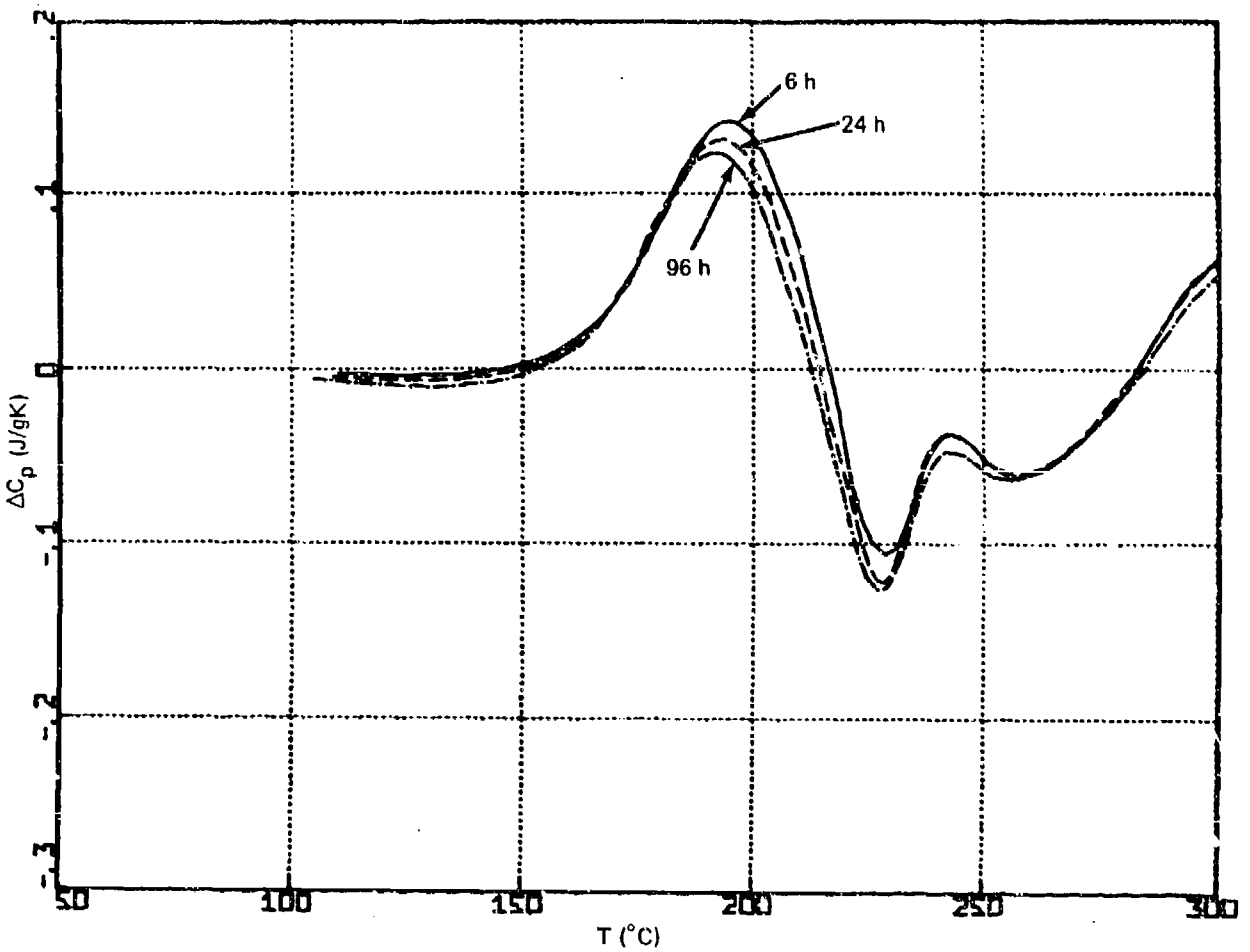

Fig. 8. DSC Traces From Solution Treated 7075 After Pre-Aging for 6, 24 and 96 Hours at 90°C and Final Aging for 8 Hours at 150°C.

Table 3. DSC Characteristics After Two Stage Aging Treatments Where Final Aging was at 150°C

Aging I		Aging II				Peak I		Peak IIa		Peak IIb	
t (h)	T (°C)	t (h)	T (°C)	Hardness (R_B)	EC (% IACS)	T_r (°C)	ΔH_r (J/g)	T_r (°C)	ΔH_r (J/g)	T_r (°C)	ΔH_r (J/g)
6	90	8	150	86±1	33.8	196	4.8±.2	229	-1.8±.2	256	-1.6±.2
24	90	8	150	84±1	33.5	195	4.3±.3	229	-2.1±.3	257	-1.7±.1
96	90	8	150	83±2	33.7	193	4.1±.3	228	-2.4±.2	254	-1.8±.1
6	120	8	150	83±3	33.7	197±2	4.1±.3	228	-1.9±.2	256	-1.9±.2
24	120	8	150	83±1	33.5	195	4.2±.4	228	-2.1±.3	253±2	-2.1±.3
96	120	8	150	82±5	33.8	195	3.8±.4	228	-1.9±.2	253±2	-2.1±.2
6	75	8	150	82±2	33.8	201	3.9±.1	230±2	-1.3±.3	260±3	-1.5±.2
6	85	8	150	83±4	33.5	194	3.7±.3	229	-2.5±.1	256	-2.3±.1
6	90	8	150	86±1	33.8	196	4.8±.2	229	-1.8±.2	256	-1.6±.2
6	95	8	150	84±2	33.4	194±2	3.5±.2	230	-2.3±.2	256	-2.3±.1
6	100	8	150	85±4	33.4	194	3.2±.3	228	-2.3±.3	254	-2.3±.1
6	105	8	150	80±1	33.9	196	4.7±.7	229	-1.7±.4	256	-1.6±.5
6	120	8	150	83±3	33.7	197±2	4.1±.3	228	-1.9±.2	256	-1.9±.2

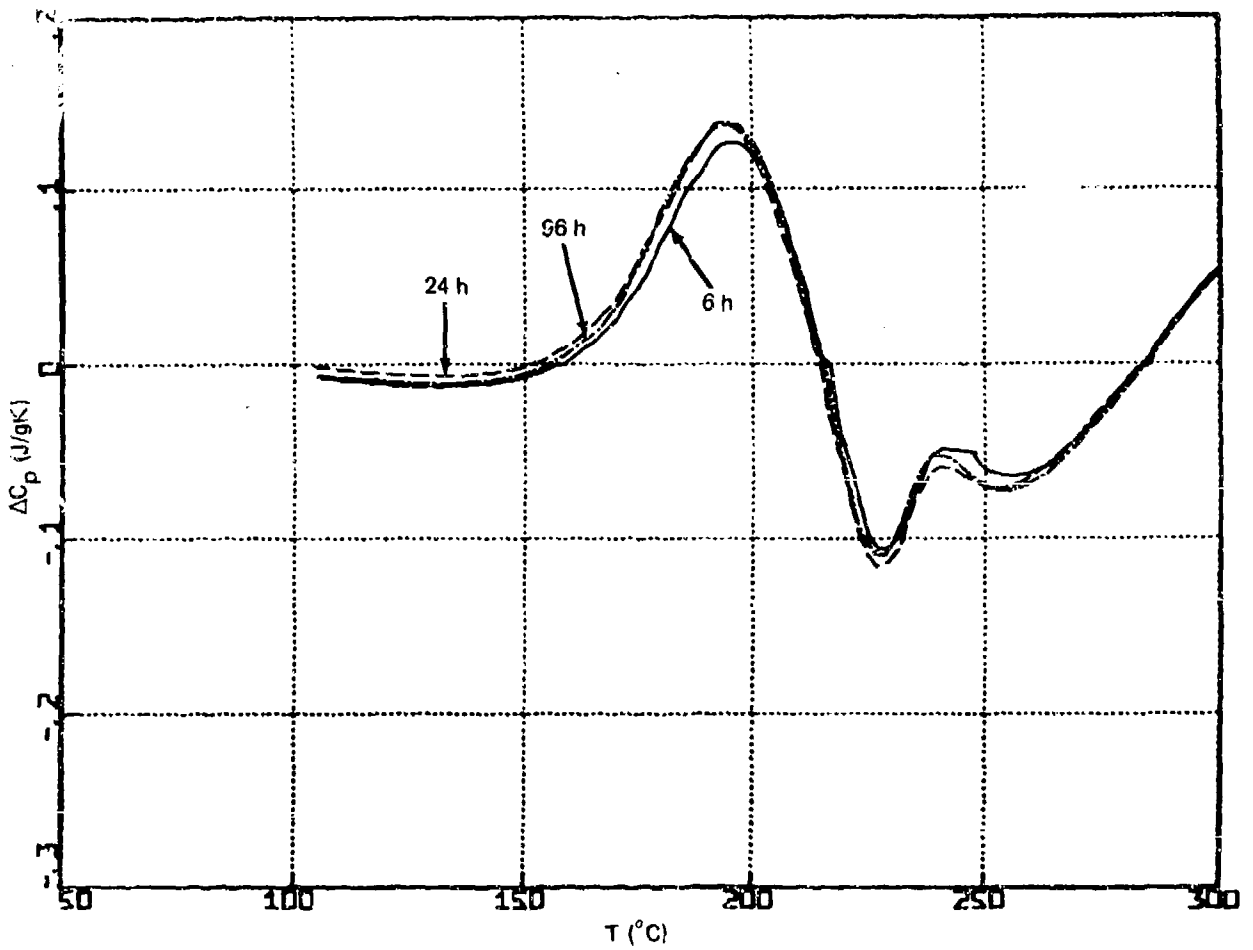

Fig. 9. DSC Traces From Solution Treated 7075 After Pre-Aging for 6, 24 and 96 Hours at 120°C and Final Aging for 8 Hours at 150°C.

ΔH_r and T_r of Peak I. No significant change occurred in either Peak II or the hardness or the conductivity.

The third set of samples in this series were first aged for 6 h at 75, 85, 90, 95, 100, 105 and 120°C and then aged for 8 h at 150°C. Results from these samples are shown in Fig. 10 and tabulated in Table 3. The sample that was first aged at 75°C displayed a significantly smaller ΔH_r for Peak II and a somewhat higher T_r for Peak I than the rest of the samples. For the remainder of the samples, the data do not seem to show any clear trends. There is some indication of a larger ΔH_r for Peak I in the sample aged at 90 or 105°C.

3.4 COMMERCIAL TYPE AGING TREATMENT

This series of aging treatments consisted of small variations in aging temperatures centered around the values recommended by the Aluminum Association.

The first series of samples were aged for 4 h at 95°C and then 8 h at 150, 155 and 160°C. The DSC results are shown in Fig. 11 and tabulated in Table 4. The results show that increasing the second aging temperature to 155 or 160°C causes a significant increase in the T_r of Peak I and a very marked decrease in ΔH_r of Peak II. The hardness and conductivity values also show this trend. Increasing the aging temperature to 155 or 160°C caused both the hardness and conductivity to increase compared to their value after aging at 150°C.

Figure 12 shows the results of aging for 4 h at 90, 95 and 100°C before aging for 8 h at 155°C. The curves in Fig. 12 indicate small differences between the microstructures, but the data in Table 4 indicate that there was no statistically significant difference between these three aging treatments. Similarly, the hardness and conductivity values do not show any significant changes.

The results from the final batch of samples in this group are shown in Fig. 13. These samples were aged for 8 h at 95, 100, 105 and 110°C before aging for 24 h at 165°C. No significant difference was observed in the DSC results or in the electrical conductivity or hardness of these samples.

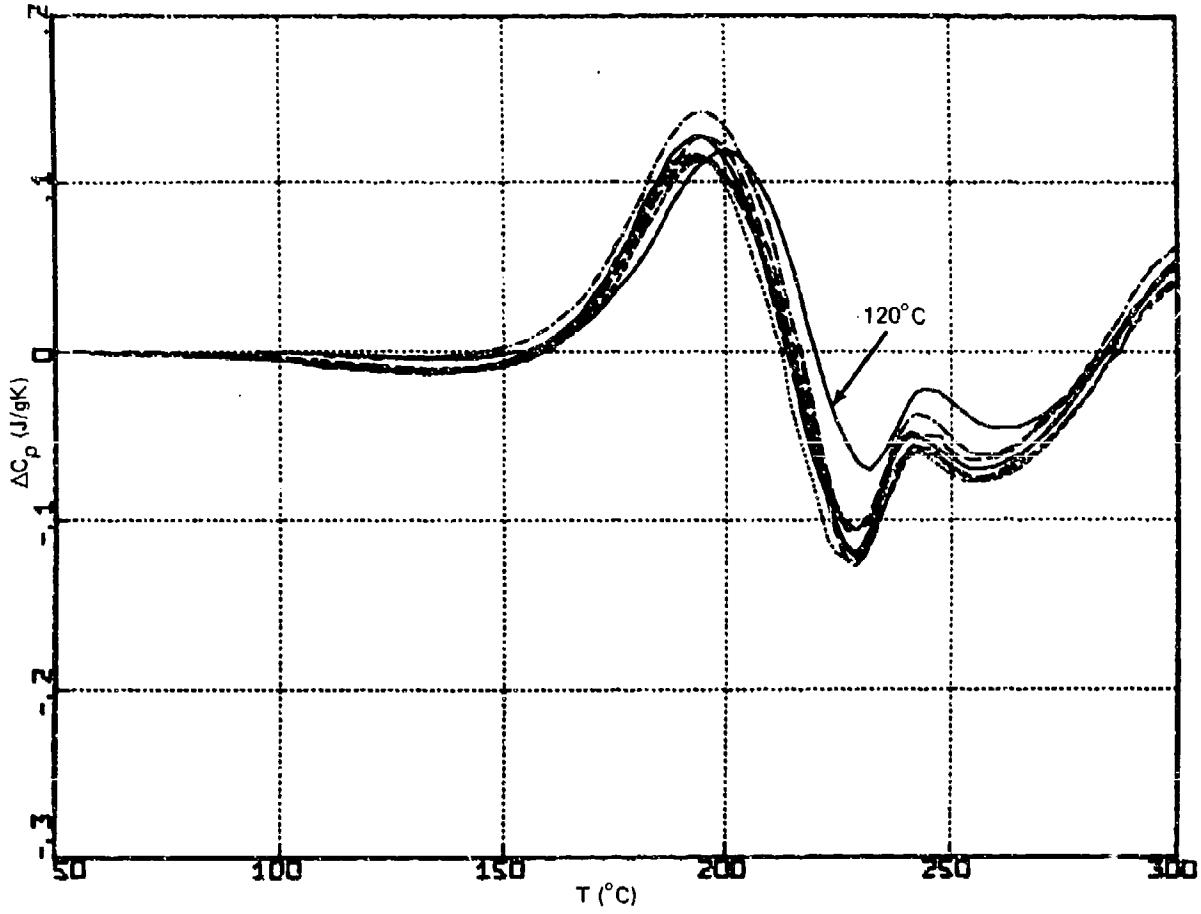

Fig. 10. DSC Traces From Solution Treated 7075 After Pre-Aging for 6 Hours at 75, 85, 90, 95, 100, 105 and 120°C and Final Aging for 8 Hours at 150°C. Most of the Curves are Very Similar and Thus Could not be Labeled.

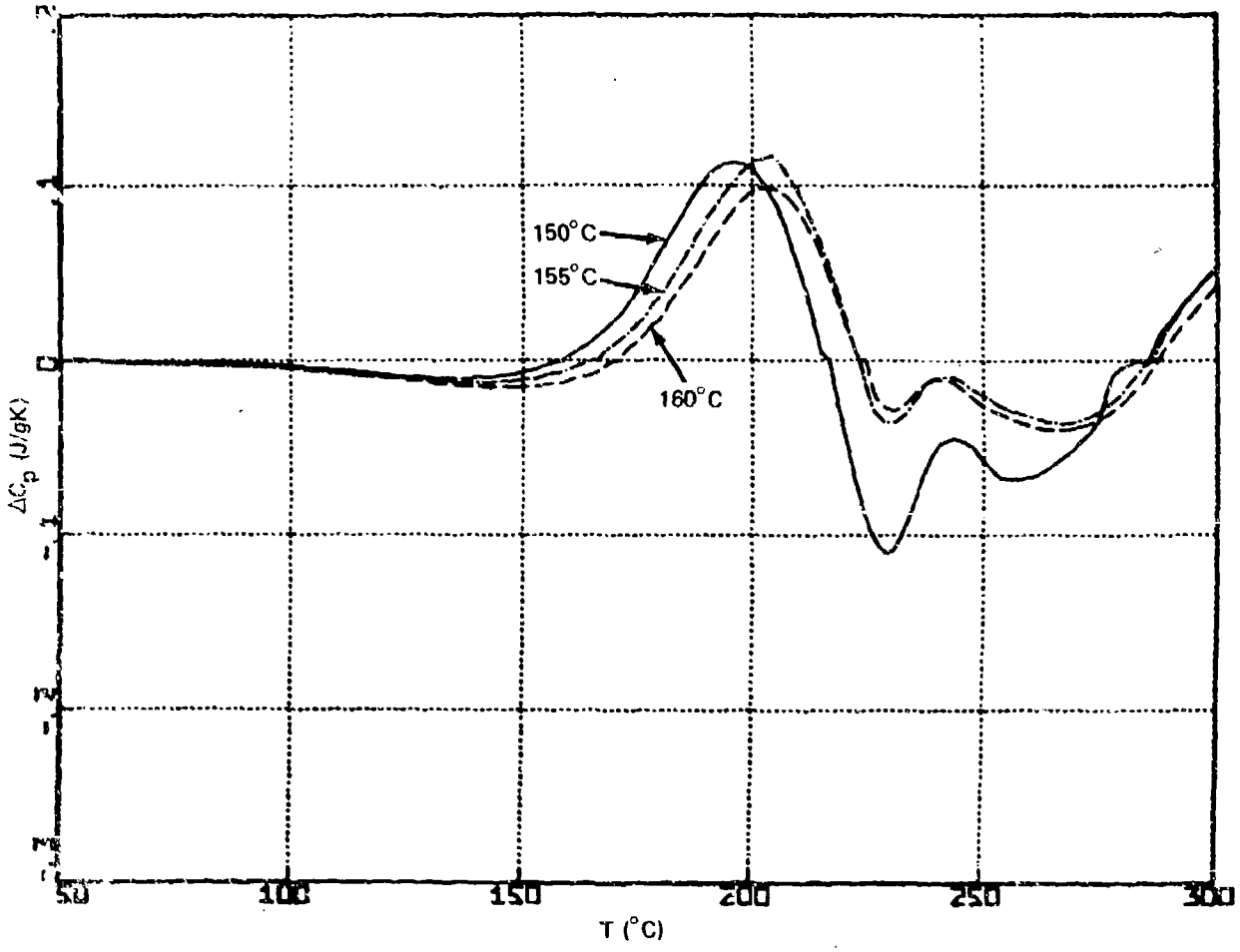

Fig. 11. DSC Traces From Solution Treated 7075 After Pre-Aging for 4 Hours at 95°C and Final Aging for 8 Hours at 150, 155 and 160°C.

Table 4. DSC Characteristics After Commercial Type Aging Treatments

Aging I		Aging II				Peak I		Peak IIa		Peak IIb	
t (h)	T (°C)	t (h)	T (°C)	Hardness (R_B)	EC (% IACS)	T_r (°C)	ΔH_r (J/g)	T_r (°C)	ΔH_r (J/g)	T_r (°C)	ΔH_r (J/g)
4	95	8	150	79±3	33.5	195±1	3.5±.1	229	-2.1±.3	255	-2.1±.2
4	95	8	155	83±4	36.0	205	3.3±.5	230	-.2±.2	263	-.9±.5
4	95	8	160	84±3	35.6	203±2	3.6±.1	230±2	-.5±.1	266±2	-1.1±.1
4	90	8	155	84±2	36.5	205±2	3.3±.5	231±2	-.1±.2	267±3	-.6±.3
4	95	8	155	83±4	36.0	205	3.3±.5	230	-.2±.2	263	-.9±.5
4	100	8	155	81±4	35.9	202±2	3.5±.5	231	-.4±.1	266±3	-1.0±.1
8	95	24	165	82±2	38.6	208	4.2±.2				
8	100	24	165	79±4	38.6	208	3.9±.1				
8	105	24	165	80±2	39.0	208	4.0±.5				
8	110	24	165	83±3	38.7	209	4.1±.1				
RRA		SURFACE		84±2		205	6.5±.1				
RRA		MID-THICKNESS		87±1		210	6.2±.2				

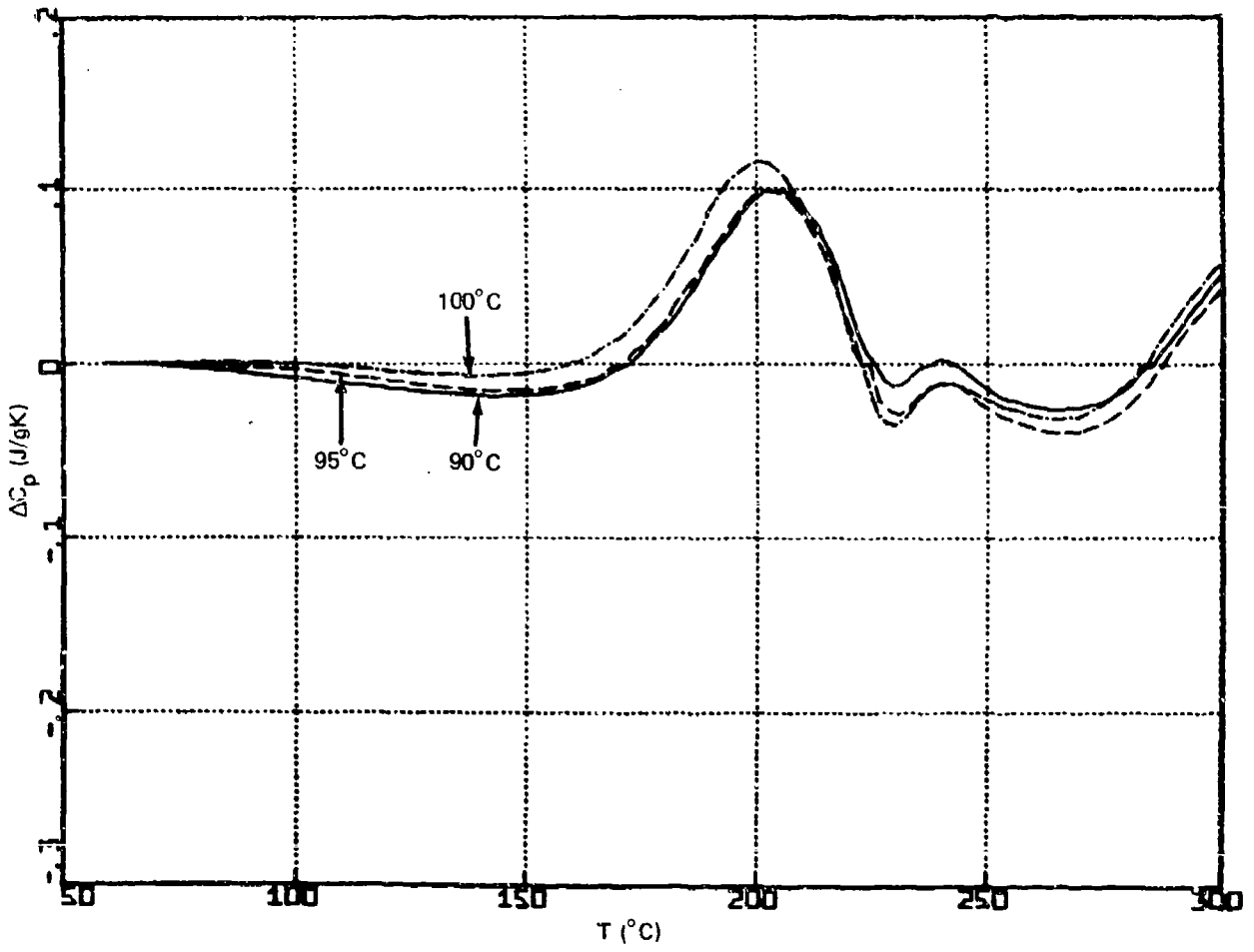

Fig. 12. DSC Traces From Solution Treated 7075 After Pre-Aging for 4 Hours at 90, 95 and 100°C and Final Aging for 8 Hours at 155°C.

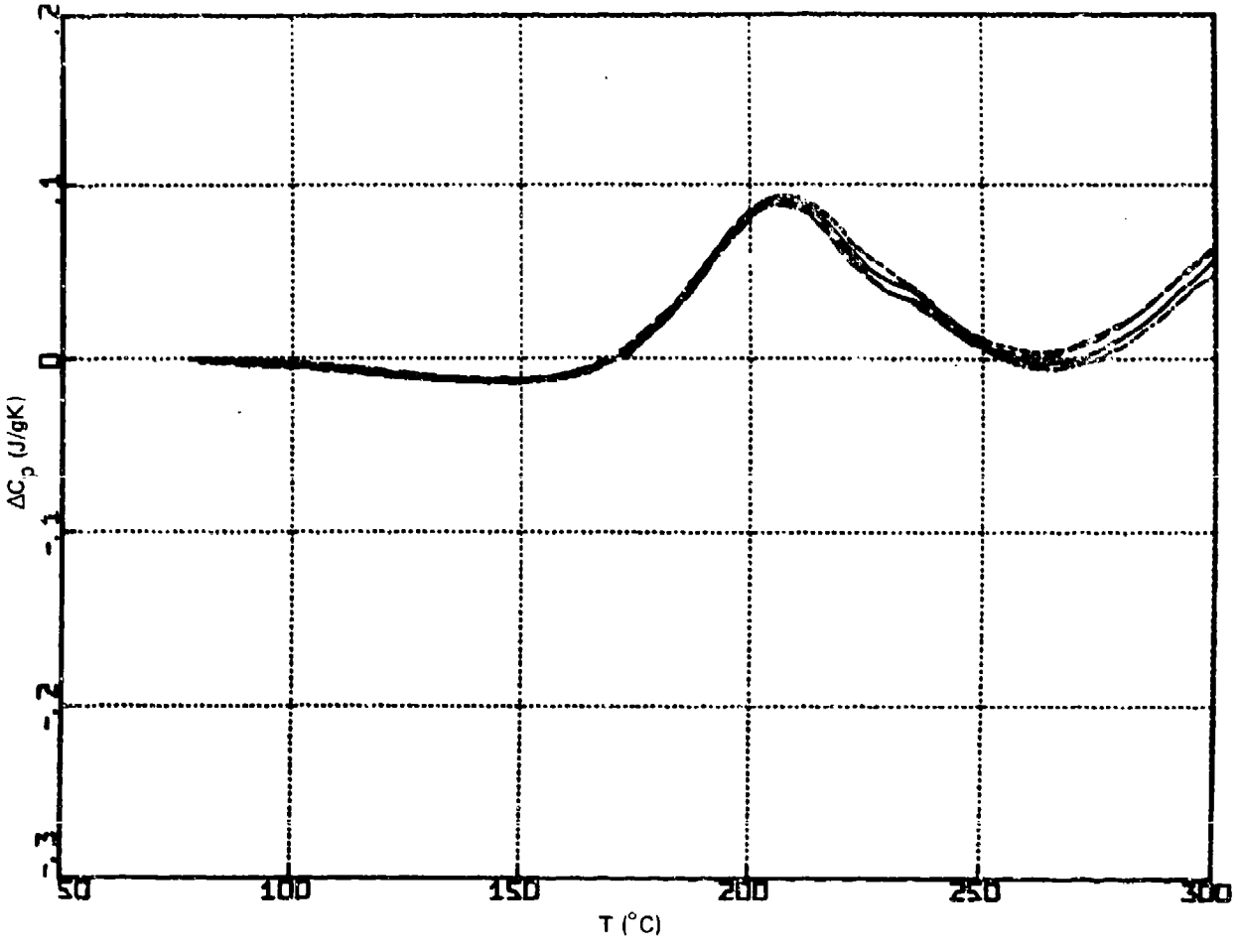

Fig. 13. DSC Traces From Solution Treated 7075 After Pre-Aging for 8 Hours at 95, 100, 105 and 110°C and Final Aging for 24 Hours at 165°C.

3.5 RETROGRESSION AND REAGING TREATMENT

Samples were taken from near the surface and at the mid-thickness of a 1 in. thick piece of 7075-T651 plate that had been RRA treated by Lockheed-California Company. The DSC results from these samples are shown in Fig. 14 and consist solely of a dissolution peak at approximately 205°C. There was little difference between the surface and the center of the sample. The shape of the DSC trace is similar to the T7 type of microstructure shown in Fig. 13, but the H_r of Peak I is significantly greater in the RRA samples.

3.6 TRANSMISSION ELECTRON MICROSCOPY RESULTS

The results of the TEM studies of grain boundary precipitates are listed in Table 5. The samples investigated had received the following aging treatments: a T6 treatment (24 h at 120°C), a two stage T6 treatment (4 h at 95°C and 8 h at 155°C), a T73 treatment (8 h at 105°C and 24 h at 165°C), and a laboratory RRA treatment of 24 h at 120°C plus 60 s at 240°C plus 24 h at 120°C. Note that this may not be the optimum RRA treatment. The data show large variations in the numbers and sizes of the precipitates between different boundaries in the same thin foil and between different thin foils from the same sample. Thus, the standard deviations listed in Table 5 are so large that it is difficult to draw conclusions. There is some indication that the T7 type of heat treatment resulted in the largest average grain boundary precipitate diameter, the largest area fraction covered and the smallest number of particles per unit area. The standard T6 aging and the RRA type of heat treatment both appeared to give similar results of smallest particle size, smallest fraction coverage and largest particle density. The two stage T6 type of aging treatment resulted in grain boundary precipitate characteristics which were intermediate between the two extremes.

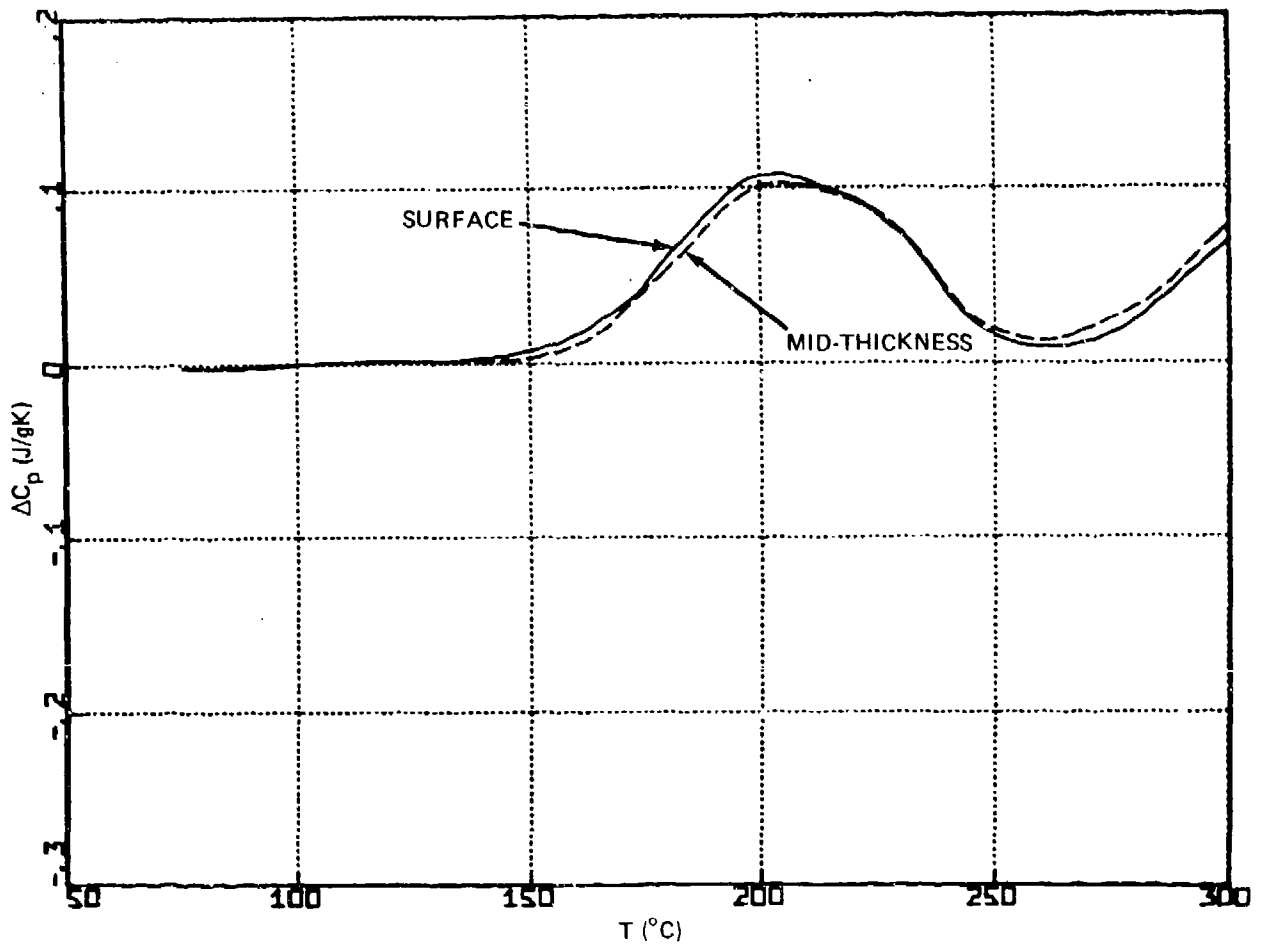

Fig. 14. DSC Traces From the Surface and Mid-Thickness of a One Inch Thick Piece of 7075-T651 that Received the Patented Retrogression and Re-Aging (RRA) Treatment.

Table 5. Characteristics of the Grain Boundary Precipitates

Temper	N	N_A $(\mu m^2)^{-1}$	$\bar{\ell}$ (nm)	A_f
T6	635	302±190	28±13	0.16±.06
Two Stage T6	401	130±80	55±19	0.23±.09
RRA*	545	372±185	34±16	0.21±.05
T73	102	80±50	66±20	0.29±.03

*Laboratory treated T6 material that was given a retrogression treatment if 60 s at 240°C and then re-aged for 24 h at 120°C.

4. DISCUSSION

The results of this program contain a great deal of information about the microstructures produced during aging of 7075. In particular, the effects of the various low temperature pre-aging treatments show a rather complex pattern of microstructural evolution. Previously published DSC studies of 7075 in which the DSC signatures were compared to the TEM microstructures dealt only with aging temperatures of 120°C or higher (Ref 5). Thus, there is no firm basis upon which to assign specific reactions to specific reaction peaks in the data. Numerous observations suggest themselves, but it would probably be misleading to speculate on the nature of these low temperature microstructures without further information. An example of the difficulty of interpreting the low temperature aging results can be found in Fig. 2 where aging for a given time at increasing temperatures results in a smaller and smaller dissolution enthalpy for Peak I. This does not necessarily indicate that less precipitate is formed at the higher temperature, but may simply show that the dissolution and formation peaks are overlapping. Without detailed knowledge of the reactions involved, further comment is not justified. The results of the two-stage aging treatments, however, show several significant trends.

The results from experiments in which pre-aging was carried out for 6, 24 and 96 h at 90 or 120°C before final aging for 8 h at 150°C show that the final microstructures were quite similar for all of these conditions. However, the dissolution enthalpy for Peak I, the strengthening precipitate, is a maximum for the shortest pre-age at the lower temperature. This dissolution enthalpy decreases regularly as the time and temperature of preaging increase. The hardness values lead to the same general conclusion, with the shortest pre-age at the lowest temperature giving the hardest structure. The microstructure produced by 6 h at 90°C plus 8 h at 150°C is very similar to the standard T6 (24 h at 120°C) both in hardness and in DSC characteristics with the exception of Peak II which was smaller in the two-stage sample. These microstructural results can be understood on the basis of the Pashley et al model for two stage aging (Ref 15) since a finer

low temperature microstructure will result in a finer final microstructure. The Lorimer and Nicholson model (Ref 14) would predict the opposite behavior, since a longer preaging treatment should result in a larger fraction of G.P. zones which can survive the up-quench and hence nucleate a finer final microstructure, which would presumably be stronger.

The results of the two-stage aging experiments in which pre-aging was carried out for 6 h at various temperatures before final aging at 150°C again show similar final microstructures, but with some trends suggested by the data. The lowest aging temperature, 75°C, when compared to the standard T6 (24 h at 120°C) appears to result in a slightly overaged, weaker microstructure since T_r for Peak I is above 200°C and ΔH_r for Peak II is significantly reduced. As the pre-aging temperature increases, the characteristics of the samples improve and then oscillate. This behavior, if it is genuine and not simply due to inaccuracies and error accumulation, can be explained on the basis of inadequate pre-aging at 75°C and, subsequently, the formation of different precipitate phases at different preaging temperatures. A change from G.P. zone microstructures to η'' microstructures in this temperature range has been documented for medium strength Al-Zn-Mg alloys (Ref 23 and 24) and suggested for 7075 (Ref 11). Clarification of the nature of the microstructures produced during the pre-aging treatments and an accurate placement of the phase boundaries would aid in understanding this result.

The results of varying the final aging temperature from 150 to 160°C show significant microstructural effects in this temperature range as shown in Fig. 11. Changing the final aging temperature from 150 to 155°C resulted in an approximately four fold decrease in the area of Peak II with only a small effect on Peak I. This result implies that the rate of formation of η' and/or η is significantly greater at 155°C than at 150°C. Increasing the temperature further to 160°C had little additional effect. Pre-aging for 4 h at 90 to 100°C with final aging of 8 h at 155 to 165°C is specified in the Aluminum Standards and Data publication (Ref 4) as an alternate means of producing the T6 temper. This result shows that increasing the final aging temperature from 150°C as suggested by DiRusso et al (Ref 1) to 155°C as recommended by the Aluminum Association (Ref 4) has a pronounced effect on the final microstructure. The effect of varying the pre-aging temperature between 90

and 100°C was not as pronounced, as can be seen in Fig. 12. The differences indicated in Fig. 12 are not supported by the actual enthalpies listed in Table 4. These results agree with the tensile data presented by Buratti et al (Ref 3). They showed that variations in the pre-aging treatment did not have much of effect on the final properties but that changing the final aging temperature caused significant shifts in the aging curves. This same observation holds true for the two-stage T73 (8 h at 105°C plus 24 h at 165°C) and T76 (8 h at 100°C plus 24 h at 165°C) type treatments shown in Fig. 13. No significant differences were observed between the characteristics of the microstructures produced by varying the pre-aging temperature between 95 and 110°C when the final aging treatment was 24 h at 165°C.

The DSC characteristics of the microstructures produced by the patented RRA treatment appear to be similar to those of the T7 type treatments. However, the dissolution enthalpy for Peak I in the RRA material is approximately 50% greater and the peak is much broader. We have observed previously in this work, and in other studies (Ref 6), that the hardness is related to the enthalpy of Peak I, thus the larger dissolution enthalpy in the RRA material is expected to result in greater hardness, as observed. These results indicate that the RRA treatment results in η' and η microstructures which are more similar to T7 microstructures than to T6, but which are harder than the η' and η microstructures produced by two stage, T7 type treatments.

The differences between the various commercially used microstructures are shown in Fig. 15. The most pronounced difference is thought to be in Peak II, the formation peak. For the T7 and RRA treatments, Peak II is absent. This indicates that these microstructures consist entirely of η' and η. The two stage T6 shows a small Peak II, while the standard T6 shows a large Peak II. Thus, while the T7 and RRA microstructures are exclusively η' and η, the two stage T6 contains less of these phases and the ordinary T6 least of all. In addition, Peak I is different in the various conditions. When compared to the ordinary T6, Peak I in the two stage T6 is broader and shifted to a higher temperature. This is indicative of a larger average particle size and/or a greater proportion of η' in the two stage microstructure. Peak I for the T7 microstructures is somewhat broader as is typical of the η' usually observed in this temper (Ref 5). This indicates a broader particle size distribution

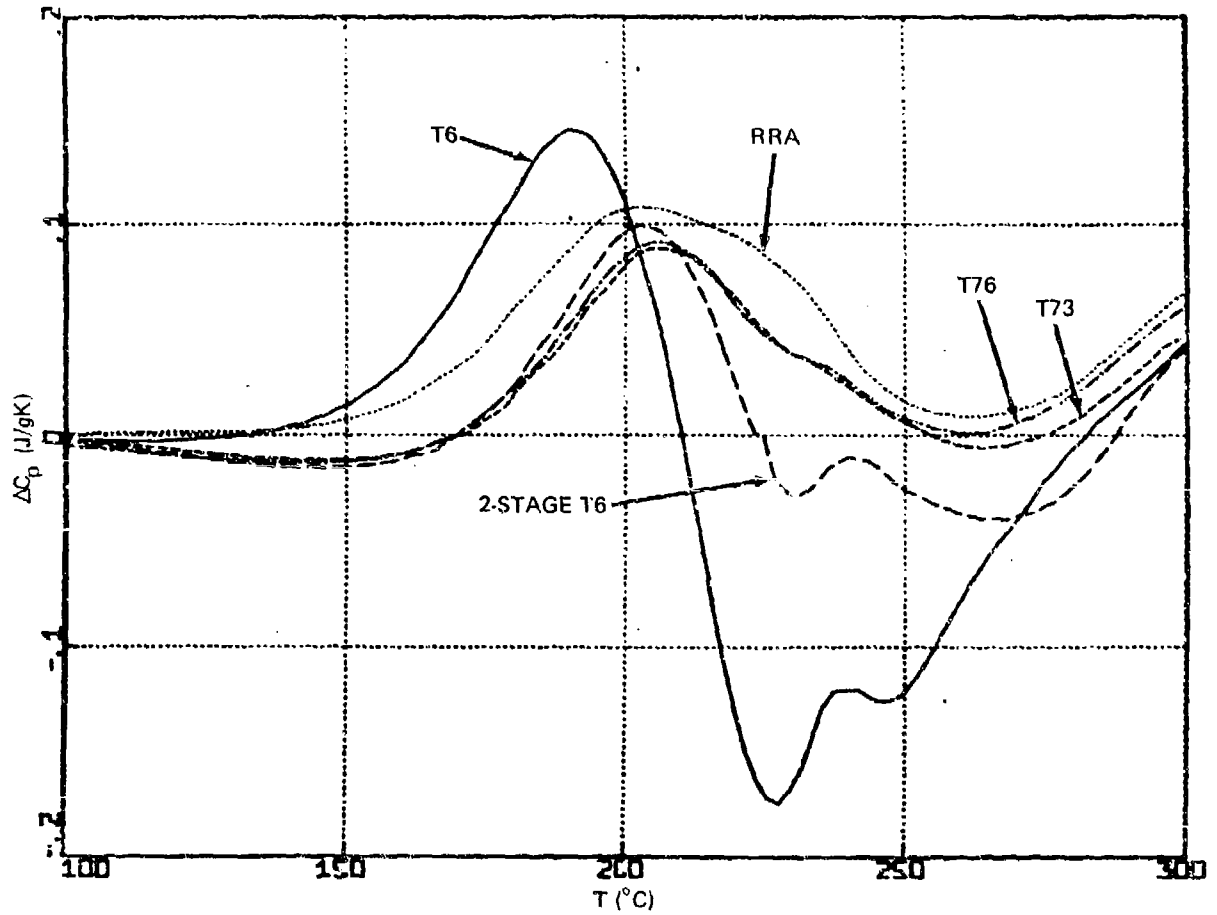

Fig. 15. DSC Traces From Solution Treated 7075 that Received a T6 Aging Treatment (24 Hours at 120°C), a Two-Stage T6 Treatment (4 Hours at 95°C and 8 Hours at 155°C), a T76 Treatment (8 Hours at 100°C and 24 Hours at 165°C) and a T73 Treatment (8 Hours at 105°C and 24 Hours at 165°C) and From a Sample of 7075-T651 Which Received the Patented RRA Treatment.

or may simply be the result of the absence of overlap with Peak II. Peak I in the RRA microstructure is broader still and appears to be a superposition of multiple dissolution peaks, suggesting that the RRA microstructure consists of a mixture of several precipitate phases. All of the tempers are mixtures of precipitate phases to some extent, but the RRA appears to contain the greatest variety.

In summary therefore, the high final aging temperature of the two stage T7 results in a predominately η' microstructure which is more coarsely distributed then those microstructures produced at lower temperatures. The two-stage T6, which receives a final aging treatment at 155°C, succeeds in conserving the relatively fine microstructure it inherits from the low temperature pre-age. The ordinary T6 contains the finest distribution of strengthening precipitates, predominately G.P. zones, but it has the least amount of more stable η' and η phases. The RRA treatment appears to dissolve the G.P. zones inherited from the T6 starting microstructure, but, since the final aging treatment is performed at 120°C, excessive coarsening of the η' and η components of the microstructure does not occur and the final result is both fine scale and stable.

The relationship of these results to the stress corrosion susceptibility of the various tempers will now be considered. Unfortunately, the stress corrosion data for these samples is not yet available, but, for the purposes of this short discussion we will assume on the basis of previously published results (Ref 1, 2, and 29) that the T7 and the RRA tempers are the most stress corrosion resistant, that the ordinary T6 is the least resistant and the two stage T6 is intermediate. Various authors have found that the stress corrosion susceptibility of Al-Zn-Mg alloys is controlled by the characteristics of the grain boundary precipitates (Ref 30 through 35), the matrix microstructure (Ref 36), or by factors related to hydrogen embrittlement (Ref 37 through 41).

If grain boundary precipitate density and size were the primary factor, then the data in Table 5 would lead us to expect best stress corrosion resistance for the T73, worst for the T6 and RRA, and intermediate resistance for the two stage T6. This is not in agreement with the previously published results for these conditions mentioned above. If matrix microstructure were of

greatest importance, then we would predict a different result. Assuming that the DSC characteristics of the T7 microstructures are the desirable characteristics for stress corrosion resistance and the DSC characteristics of the T6 microstructure are the undesirable ones, then we would predict that the RRA should have a stress corrosion resistance equivalent to that of the T7. This prediction is based on the enthalpy of Peak II, which is absent in the T7 and RRA microstructures and which is maximum for the T6. The two stage T6 would be expected to have intermediate stress corrosion resistance on this basis. This prediction agrees with the expected ranking mentioned above.

Recent work on stress corrosion has emphasized the role of hydrogen, in particular, the effects of magnesium segregated to grain boundaries (Ref 41 and 42) and the role of grain boundary precipitates (Ref 40). If magnesium segregation is of primary importance, and if it is assumed that the segregation is of the non-equilibrium, vacancy aided type which occurs during quenching (Ref 43 and 44), then aging at elevated temperatures will allow re-establishment of equilibrium solute partitioning by diffusion. Rough calculations of the root mean square diffusion distance of magnesium during the aging treatments indicate that the T7 allows the greatest diffusion distance, the RRA allows approximately 80% as much, the two-stage T6 allows 35% as much, and the T6 only allows 10% as much. Thus, this theory correctly predicts the expected ranking. Finally, Christodoulou and Flower (Ref 40) have found that grain boundary n particles larger than 20 nm are effective as nucleation sites for hydrogen bubbles, and thus decrease the amount of hydrogen dissolved in the matrix and grain boundaries thereby reducing the stress corrosion susceptibility. Our characterization of the grain boundary precipitates was not quantitative enough to determine the relative fraction of precipitates greater than 20 nm, thus our data do not allow comparison to this theory.

5. SUMMARY

1. For two-stage aging treatments in which the final aging is for 8 h at 150°C, pre-aging for 6 h at 90°C produces a slightly finer and harder microstructure than longer treatments at 90°C or equivalent treatments at 120°C. This is in agreement with the Pashley et al model of two-stage aging.

2. For two-stage treatments where the first aging treatment is 4 h at 95°C, increasing the final aging temperature from 150 to 155 or 160°C results in a significant increase in the amount of η' in the microstructure. Variations in the pre-aging treatment had much less of an effect.

3. The RRA heat treaqtment converts the T6, predominately G.P. zone microstructure, to a more stable T7 type of microstructure; but the RRA microstructure consists of smaller precipitates and is more heterogeneous than the T7.

4. The major differences between the T6, two-stage T6, RRA and T73 microstructures appear to be in the relative proportions of G.P. zones, η' and η. The percentage of G.P. zones is greatest in T6, least in T73 and RRA and intermediate in the two-stage T6.

5. The stress corrosion susceptibility of 7075 appears to be more influenced by the matrix microstructure than by the grain boundary precipitate size and spacing.

6. RECOMMENDATIONS FOR FUTURE WORK

The observations made in the course of this work have raised several technical issues which should be addressed in order to complement the experiments already performed and to maximize the scientific benefit of this effort. They are:

1. Comparison stress corrosion testing of the four commercial tempers, (T6, two-stage T6, T73 and RRA) should be performed. The results of these stress corrosion tests are necessary for interpretation of the DSC results obtained in this work. The two-stage T6 should not be overlooked in the stress corrosion testing. As shown in the discussion, stress corrosion data from the two-stage T6 condition is a key factor in the separation of the various microstructural effects that have been observed, and would be of great utility in determining which particular microstructural characteristic is of greatest significance in the stress corrosion behavior of 7075 in a high strength condition.

2. Additional DSC studies of the microstructures in the various stages of the RRA treatment in 7075 should be performed and correlated with stress corrosion behavior. As shown in our progress report, DSC is a very rapid and sensitive indicator of the extent of retrogression and, as such, it can be of great use in establishing the correct processing condtions for a particular part. Once the optimum microstructural conditions after retrogression and after reaging are established, these data could be used for rapid and precise determination of procesing parameters for parts of different thicknesses, geometries or prior microstructural conditions.

3. DSC studies of the various stages of RRA treatments in 7050 should be performed and correlated with stress corrosion testing. Since the T6 microstructure of 7050 has a DSC signature which closely resembles that of the two-stage T6 in 7075, it is expected that RRA may provide less improvement in the stress corrosion behavior of 7050 than of

7075. Data from these tests would allow generalization of the conclusions about the relationship between microstructure and stress corrosion susceptibility in 7075 to the 7000 series.

4. Additional TEM studies should be performed to establish the precise identity of the precipitates formed during low temperature aging of 7075, and these data should be correlated with the DSC results in order to allow a better understanding of the structures obtained in the pre-aging treatments and to enhance the utility of the DSC technique.

5. Quantitative transmission electron microscopy studies using dark field techniques should be performed in samples representative of the four commercial type aging treatments. The objectives of this work would be to quantitatively determine the number density and size distribution of the G.P. zones, η'', η' and η precipitates both in the matrix and grain boundaries of the four microstructures. The results of this study when compared with stress corrosion and mechanical property data will establish the precise microstructural conditions which lead to best properties and should allow even further microstructural optimization.

7. REFERRENCES

1. E. DiRusso, M. Conserva, F. Gatto and H. Markus, "Thermomechanical Treatments on High Strength Al-Zn-Mg (-Cu) Alloys," Met Trans, Vol 4, p 1133, 1973.

2. R.S. Kaneko, "RRA: Solution for Stress Corrosion Problems with T6 Temper Aluminum," Metals Progress, Vol 117, No. 5, p 41, April 1980.

3. M. Buratti, C. Arcolin and E. DiRusso, "Indagini Sui Cicli Di Invecchiamento Artificiale a Due Stade die Leghe Commerciali Al-Zn-Mg-Cu-Cr," Aluminio, Vol 42, No. 1, p 40, 1973.

4. Aluminum Standards and Data 1978 Metric SI, The Aluminum Association, Inc., 818 Connecticut Ave, N.W., Washington, DC 10006, 1978.

5. R. Delasi and P.N. Adler, "Calorimetric Studies of 7000 Series Aluminum Alloys: I. Matrix Precipitate Characterization of 7075," Met Trans, Vol 8A, p 1177, 1977.

6. P.N. Adler and R. Delasi, " Calorimetric Studies of 7000 Series Auminum Alloys: II. Comparison of 7075, 7050 and RX720 Alloys," Met Trans, Vol 8A, p 1185, 1977.

7. A. Kelly and R.B. Nicholson, "Precipitation Hardening," Progress in Materials Science, Vol 10, p 149, 1963.

8. J. Gjønnes and Chr. J. Siemenson, "An Electron Microscope Investigation of the Microstructure in an Aluminum - Zinc - Magnesium Alloy," Acta Met, Vol 18, p 881, 1970.

9. C.E. Lyman and J.B. Vander Sande, " A Transmission Electron Microscopy Investigation of the Early Stages of Precipitation in an Al-Zn-Mg Alloy," Met Trans A, Vol 7A, p 1211, 1976.

10. G.W. Lorimer, "Precipitation in Aluminum alloys," in "Precipitation Processes in Solids," edited by K.C. Russel and H.I. Aaronson, TMS-AIME, Warrendale, PA, 1978.

11. R.J. Rioja, K.J. Brunner and D.E. Laughlin, "Early Stages of Precipitation in a Al-Zn-Mg Alloy," presented at the Fall meeting TMS-AIME, J. of Metals, Vol 32, No. 8, p 34, 1980.

12. L.F. Mondoyo, N.A. Gjostein and D.W. Levinson, "Structural Changes During the Aging in an Al-Zn-Mg Alloy," Trans AIME, Vol 206, Sec. 2, p 1378, 1956.

13. A.J. DeArdo, Jr. and Chr. J. Simensen, "A Structural Investigation of Multiple Aging of Al-7% Zn-2.3% Mg," Met Trans, Vol 4, p 2413, 1973.

14. G.W. Lorimer and R.B. Nicholson, The Mechanism of Phase Transformation in Crystalline Solids, Inst of Metals, London, p 36, 1968.

15. D.W. Pashley, M.H. Jacobs, and J.T. Vietz, "The Basic Processes Affecting Two-Step Aging in an Al-Mg-Si Alloy," Phil. Mag., Vol 16, p 51, 1967.

16. K. Asano and K. Hirano, "Precipitation Process in an Al-Zn-Mg Alloy," Trans Japan Inst of Metals, Vol 9, p 24, 1968.

17. K. Asano and K. Hirano, "Two-Step Aging in an Aluminum 5 wt% Zinc - 1 wt% Magnesium alloy," Trans Japan Inst of Metals, Vol 9, p 149, 1968.

18. K. Hirano and K. Asano, "Prolonged Aging of an Aluminum-Zinc-Magnesium Alloy," Trans Japan Inst of Metals, Vol 11, p 225, 1970.

19. A. Zahra, C.Y. Zahra, M. Lafitte, W. Lacom and H.P. Degischer, "Entmischungsvorgange in einer Al-5% Zn-1% Mg-Legierung, Teil I: Kalorimetrische Untersuchungen," Z. Metallkde, Vol 70, p 172, 1979.

20. D.S. Thompson, "The Calorimetric Observations of Solid State Reactions in Aluminum alloys," in Thermal Analysis, Vol 2, p 1147, Academic Press, 1969.

21. G. Groma, E. Kovacs-Csetenyi, I. Kovacs, J. Lendvai and T. Ungar, "The Composition of Guinier-Preston Zones in Al-Zn-Mg Alloys," Philos Mag. A, Vol 40, p 653, 1979.

22. J. Lendvai, Gy. Honyek and I. Kovacs, "Dissolution of Second Phases in an Al-Zn-Mg Alloy Investigated by Calorimetric Method," Scripta Met., Vol 13, p 593, 1979.

23. T. Ungar, "The Formation of Gunier-Preston Zones in the Al-4.8 wt% Zn-1.2 wt% Mg Alloy Studied by X-Ray Small Angle Scattering," Zeit. Metallkde, Vol 70, p 739, 1979.

24. H.Y. Hunsicker, "The Metallurgy of Heat Treatment," in Aluminum, Vol 1, edited by K.R. VanHorn, ASM, Metal Park, Ohio, 1967.

25. L.F. Mondolfo, "Aluminum Alloys Structure and Properties," Butterworths, London-Boston, 1976.

26. J.T. Healey and R.W. Gould, "The Effect of Thermal and Mechanical Pretreatments on the Gunier-Peston Zone State of a Commercial 7075 Alloy," Met Trans, Vol 8A, p 1907, 1977.

27. S. Ceresara and P. Fiorini, "Resistometric Investigation of the Aging Process After Quenching and Cold-Work in Al-Zn-Mg Alloys," Mater Sci Eng, Vol 10, p 205, 1972.

28. J.T. Staley, "Aging Kinetics of Aluminum Alloy 7050," Met Trans, Vol 5, p 929, 1974.

29. M.O. Speidel, "Stress Corrosion Cracking of Aluminum Alloys," Met Trans, Vol 6A, p 631, 1975.

30. K.G. Kent, "The Effect of Quench Rate on the Microstructure and Stress-Corrosion Resistance of a Weldable Al-Zn-Mg Alloy," J. Inst of Metals, Vol 97, p 127, 1969.

31. K.G. Kent, "Microstructure and Stress Corrosion Resistance of Al-Zn-Mg Alloys," J. Australian Inst of Metals, Vol 15, p 171, 1970.

32. P.N. Adler, R. DeIasi and G. Geschwind, "Influence of Microstructure on the Mechanical Properties and Stress-Corrosion Susceptibility of 7075 Aluminum Alloy," Met Trans, Vol 3, p 3191, 1972.

33. P.N. Adler and R. DeIasi, "Avoidance of Stress-Corrosion Susceptibility in High Strength Aluminum Alloys by Control of Grain Boundary and Matrix Microstructure," Final Report on NASA Contract NAS 8-28986, Grumman Research Report RE-468, Grumman Aerospace Corporation, Bethpage, NY, Jan 1974.

34. P.K. Poulose, J.E. Morral and A.J. McEvily, "Stress-Corrosion Crack Velocity and Grain Boundary Precipitates in an Al-Zn-Mg Alloy," Met Trans, Vol 5, 1393, 1974.

35. J.A.S. Green and W.G. Montague, "Observations on the Stress-Corrosion Cracking of an Al-5% Zn-2.5% Mg Ternary and Various Quaternary Alloys," Corrosion, Vol 31, No. 6, p 209, 1975.

36. A.J. DeArdo, Jr and R.D. Townsend, "The Effect of Microstructure on the Stress-Corrosion Susceptibility of a High-Purity Al-Zn-Mg Alloy in a NaCl Solution," Met Trans, Vol 1, p 2573, 1970.

37. L. Montgrain and P.R. Swann, "Electron Microscopy of Hydrogen Embrittlement in a High Purity Al-Zn-Mg Alloy," in Hydrogen in Metals, I.M. Bernstein and A.W. Thompson, p 575, ASM, Metals Park, Ohio, 1974.

38. E.C. Pow, J.C. Schwanebeck and W.W. Gerberich, "Hydrogen Effects and Cadmium Segregtion to Grain Boundaries in 7075-T6 Aluminum," Met Trans, Vol 9A, p 1009, 1978.

39. L. Christodoulou and H.M. Flower, "Hydrogen Embrittlement and Trapping in Al-6% Zn-3% Mg," Acta Met, Vol 28, p 481, 1980.

40. L. Christodoulou and H.M. Flower, "High Voltage Electron Microscopy of Hydrogen Embrittlement and Trapping in Al-Zn-Mg Alloys," Inst Phys Conf Series No. 52, Chapter 6, p 313, 1980.

41. G.M. Scamans and A.S. Rehal, "Electron Metallography of the Aluminum-Water Vapor Reaction and Its Relevance to Stress-Corrosion Susceptibility," J. Mater Sci, Vol 14, p 2459, 1979.

42. A. Csanady and D. Marton, "Stress Corrosion Behavior of Al-Zn-Mg Alloys Based Upon Microchemical Surface Reactions," J. Mater Sci, Vol 14, p 2789, 1979.

43. T.R. Anthony and R.E. Hanneman, "Non-Equilibrium Segregation of Impurities in Quenched Dilute Alloys," Scripta Met, Vol 2, p 611, 1968.

44. K.T. Aust, R.E. Hanneman, P. Niessen and J.H. Westbrook, "Solute Induced Hardening Near Grain Boundaries in Zone Refined Metals," Acta Met, Vol 16, p 291, 1968.

DISTRIBUTION LIST
(One copy unless otherwise noted)

(1 copy + balance after distribution)

Mr. Michael D. Valentine
AIR-5163C4
Naval Air Systems Command
Washington, DC 20361

Commander
Naval Air Development Center
(Code 302)
Warminster, PA 18974

Naval Sea Systems Command
(Code 03423)
Department of the Navy
Washington, DC 10360

Naval Ships Research &
Development Center
(Code 2812)
Annapolis, MD 21402

Commander
Naval Surface Weapons Center
(Metallurgy Division)
White Oak
Silver Spring, MD 20910

Director, Naval Research
Laboratory
(Codes: 6380, 6490, 6601,
8430 - 1 copy each)
Washington, DC 20390

Office of Naval Research
The Metallurgy Program
Code 471
Arlington, VA 22217

Dr. T.R. McNelley
Department of Mechanical
Engineering (Code 59)
Naval Posgraduate School
Monterey, CA 93940

14 copies (12 copies for DDC, 2
copies for AIR-954)
Commander, Naval Air Systems
Command
AIR-954
Washington, DC 20361

Wright-Patterson Air Force Base
Ohio 45433
Attn: W. Griffith, AFML/LLS

Wright-Patterson Air Force Base
Ohio 45422
Attn: C.L. Harmsworth-AFML/MXE

Army Materials & Mechanics
Research Center
Watertown, MA 02172
Attn: Dr. A. Gorum

Commanding Officer
Office of Ordnance Research
Box CM, Duke Station
Durham, North Carolina 27706

U.S. Army Armament R&D Command
(ARRADCOM)
Dover, New Jersey 07801
Attn: Dr. J. Waldman
DRDAR-SCM-P, Bldg 3409

National Aeronautics & Space
Administration
(Code RWM)
600 Independence Ave., S.W.
Washington, DC 20546

National Aeronautics & Space Administration
George C. Marshall Space Flight Center
Huntsville, Alabama 35812
Attn: Mr. H.F. Hardrath
Stop 188M

National Aeronautics & Space Administration
George C. Marshall Space Flight Center
Huntsville, Alabama 35812
Attn: Mr. J.G. Williamson
S&E-ASTN-MMC

National Academy of Sciences
Materials Advisory Board
Washington, DC 20418
Attn: Dr. J. Lane

Director
National Bureau of Standards
Washington, DC 20234
Attn: Dr. E. Passaglia

Battelle Memorial Institute
505 King Avenue
Columbus, Ohio 43201
Attn: Mr. Stephan A. Rubin
Manager, Information Operations

IIT Research Institute
Metals Research Department
10 West 35th Street
Chicago, Illinois 60616
Attn: Dr. N. Parikh

General Dynamics Convair Div.
P.O. Box 80847
San Diego, California 92138
Attn: Mr. Jack Christian
Code 643-10

Kaman Aerospace Corporation
Old Windsor Road
Bloomfield, Connecticut 06001
Attn: Mr. M.L. White

Rockwell International
Columbus Division
Columbus, Ohio 43216
Attn: Mr. P. Maynard, Dept. 75
Group 521

Rockwell International
Rocketdyne Division
Canoga Park, California 91305
Attn: Dr. Al Jacobs
Group Scientist
Materials Branch

Rockwell International
Los Angeles Division
International Airport
Los Angeles, California 90009
Attn: Gary Keller
Materials Applications

Lockheed Palo Alto Research Laboratories
Materials Science Laboratory
3251 Hanover Street
Palo Alto, California 94303
Attn: Dr. Frank A. Crossley
52-31/204

DISTRIBUTION LIST cont'd

Lockheed California Company
P.O. Box 551
Burbank, California 91503
Attn: Mr. J.M. VanOrden
Dept. 74-71, Bldg. 221,
Plant 2

Lockheed-Georgia Company
Marietta, Georgia 30061
Attn: E. Bateh

Lockheed Missile & Space Corp.
Box 504
Sunnyvale, California 94088
Attn: Mr. G. Pinkerton
Bldg. 154, Dept. 8122
Mr. C.D. McIntyre
Bldg. 182, Dept. 84-13
(1 each)

Douglas Aircraft Company
3855 Lakewood Boulevard
Long Beach, California 90808
Attn: Mr. Fred Mehe, C1-250

Sikorsky Aircraft
Division of United Aircraft
Corporation
Stratford, Connecticut 06497
Attn: Materials Department

Boeing-Vertol Company
Boeing Center
P.O. Box 16858
Philadelphia, PA 19142
Attn: Mr. J.M. Clark

The Boeing Company
Commerical Airplane
ORG. 6-8733, MS77-18
P.O. Box 3707
Seattle, Washington 98124
Attn: Cecil E. Parsons

Northrop Corporation
Aircraft Division
Dept. 3771-62
3901 West Broadway
Hawthorne, California 90250
Attn: Mr. Allen Freedman

Vought Corporation
P.O. Box 5907
Dallas, Texas 75222
Attn: Mr. A. Hohman

McDonnell Aircraft Company
St. Louis, Missouri 63166
Attn: Mr. H.J. Siegel
Materials & Processes Div
General Engineering Div

Lycoming Division
AVCO Corporation
Stratford, Connecticut 06497
Attn: Mr. Barry Goldblatt

Detroit Diesel Allison Division
General Motors Corporation
Materials Laboratories
Indianapolis, Indiana 46206

AiResearch Manufacturing
Company of America
Sky Harbor Aircraft
402 S. 36th Street
Phoenix, Arizona 85034
Attn: Mr. Jack D. Tree,
Dept. 93-35-5M

General Electric Company
Aircraft Engine Group
Materials & Processes
Technology Laboratories
Evandale, Ohio 45215

DISTRIBUTION LIST cont'd

Solar
2200 Pacific Highway
San Diego, California 92112
Attn: Dr. A. Metcalfe

Teledyne CAE
1330 Laskey Road
Toledo, Ohio 43601

Dr. Charles Gilmore
Tompkins Hall
George Washington University
Washington, DC 20006

Dr. Michael Hyatt
The Boeing Company
P.O. Box 707
Seattle, Washington 98124

General Electric Company
Corporate Research &
Development
P.O. Box 8
Schenectady, New York 12301
Attn: Dr. D. Wood

Westinghouse Electric Company
Materials & Processing
Laboratories
Beulah Road
Pittsburgh, PA 152335
Attn: Don E. Harrison

Dr. John D. Wood
Associate Professor
Lehigh University
Bethlehem, Pennsylvania 18015

General Dynamics Corporation
Convair Aerospace Division
Forth Worth Operation
P.O. Box 748
Fort Worth, Texas 76101
Attn: Tom Coyle

Dr. A.I. Mlavsky
Senior Vice President for
Technology & Director of
Corporate Technology Center
Tyco Laboratories, Inc.
16 Hickory Drive
Waltham, Massachusetts 02145

Martin Marietta Aluminum
19200 South Western Avenue
Torrance, California 90509
Attn: Mr. Paul E. Anderson
(M/C 5401)

Dr. Howard Bomberger
Reactive Metals, Inc.
Niles, Ohio 44446

Mr. W. Spurr
The Boeing Company
12842 72nd Avenue, N.E.
Kirkland, Washington 98033

Dr. John A. Schey
Department of Materials
Engineering
University of Illinois at
Chicago Circle
Box 4348
Chicago, Illinois 60680

Rockwell International
P.O. Box 1082
1027 Camino Dos Rios
Thousand Oaks, CA 91320

Pratt & Whitney Aircraft
Division of United Technologies
Florida Research and
Development Center
P.O. Box 2691
West Palm Beach, Florida 33402

DISTRIBUTION LIST cont'd

P.R. Mallory & Co., Inc.
3029 East Washington Street
Indainapolis, Indiana 46206
Attn: Technical Librarian

Martin Marietta Corporation
P.O. Box 5837
Orlando, Florida 32805
Attn: Dr. Richard C. Hall
Mail Point 275

Southwest Research Institute
8500 Culebra Road
P.O. Box 28510
San Antonio, Texas 78284
Attn: Dr. C. Gerald Gardner

Avco Space Systems Division
Lowell Industrial Park
Lowell, Massachusetts 01851

Brush Wellman, Inc.
17876 St. Clair Avenue
Clevland, Ohio 44110
Attn: Mr. Bryce King

General Electric Missile and
Space Division
Materials Science Section
P.O. Box 8555
Philadelphia, Pennsylvania
91901
Attn: Technical Library

Kawecki Berylco Industries
P.O. Box 1462
Reading, Pennsylvania 19603

Linde Company
Division of Union Carbide
P.O Box 44
Tonawanda, New York 14152

Midwest Research Institute
425 Volker Boulevard
Kansas City, Missouri 64110

University of California
Lawrence Radiation Laboratory
P.O. Box 808
Livermore, California 94550
Attn: Mr. L.W. Roberts

ERDA Division of Reactor
Development and Technology
Washington, DC 20545
Attn: Mr. J.M. Simmons, Chief
Metallurgy Section

Dr. W.C. Setzer, Director
Metallurgy & Surface Technology
Consolidated Aluminum
Corporation
P.O. Box 14448
St. Louis, MO 63178

Kaiser Aluminum & Chemical
Corporation
Aluminum Division Research
Center for Technology
P.O. Box 870
Pleasanton, California 94566
Attn: T.R. Prichett

Reynolds Metals Company
Metallurgical Research Division
4th & Canal Streets
Richmond, VA 23219
Attn: Dr. J.H. Dedrick

The Dow Metal Products Company
Hopkins Building
Midland, Michigan 48640

DISTRIBUTION LIST cont'd

Dr. F.N. Mandigo
Olin Metals Research
Laboratories
91 Shelton Avenue
New Haven, CT 06515

Dr. D.J. Duquette
Materials Engineering
Department
RPI
Troy, New York 12181

General Electric Company
Corporate Research &
Development
Building 36-441
Schenectady, New York 12345
Attn: Dr. J.H. Westbrook,
Manager
Materials Information
Services

United Technologies Research
Laboratories
East Hartford, CT 06108
Attn: Mr. Roy Fanti

Dr. E.A. Starke, Jr.
School of Chemical Engineering
and Metallurgy
Georgia Institute of Technology
Atlanta, Georgia 30332

Autonetics Division of Rockwell
International
P.O. Box 4173
Anaheim, California 92803
Attn: Mr. A.G. Gross, Jr.
Dept. 522-92

Dr. R. Balluffi, Chairman
Department of Materials Science
and Engineering
Bard Hall
Cornell University
Ithaca, New York 14853